Viscosity and Density of Isobutane Measured in Wide Ranges of Temperature and Pressure Including the Near-Critical Region

Sebastian Herrmann
Fachgebiet Technische Thermodynamik, Hochschule Zittau/Görlitz, Theodor-Körner-Allee 16, D-02763 Zittau, Germany

Egon Hassel
Lehrstuhl für Technische Thermodynamik, Universität Rostock, Albert-Einstein-Str. 2, D-18059 Rostock, Germany

Eckhard Vogel
Institut für Chemie, Universität Rostock, Albert-Einstein-Str. 3a, D-18059 Rostock, Germany

DOI 10.1002/aic.14759
Published online March 2, 2015 in Wiley Online Library (wileyonlinelibrary.com)

Accurate ηρpT data for isobutane were measured for nine isotherms between 298.15 and 498.15 K using simultaneously a vibrating-wire viscometer and a single-sinker densimeter. The maximum pressure was 93% of the saturated for subcritical isotherms and 30 MPa for supercritical isotherms. The density measurements are generally characterized by an uncertainty of ≤0.1%. Allocation errors for temperature and pressure influence significantly their uncertainty in the near-critical region. A comparison with the equation of state by Bücker and Wagner shows agreement normally within ±0.1%. The near-critical isotherm 410.15 K reveals differences to −3.7% exceeding the uncertainty of 1.9%. The uncertainty in viscosity is ≤0.3%. The comparison with the correlation of Vogel et al. yields deviations exceeding the uncertainty of the correlation (3%). The critical enhancement becomes evident for the near-critical isotherm amounting to 1.4%. The new data will improve the viscosity surface correlation. © 2015 American Institute of Chemical Engineers *AIChE J*, 61: 3116–3137, 2015

Keywords: density, viscosity, measurement, isobutane, single-sinker densimeter, vibrating-wire viscometer, near-critical region

Introduction

Isobutane is a constituent of oil and natural gas and an important working fluid in the petrochemistry industry. It is utilized as power gas in aerosols, together with normal butane, and in its liquified state as fuel gas, together with propane. Furthermore, it is used as refrigerant in the cooling industry, named R-600a, because of its low global warming and negligible ozone depletion potentials. Reliable thermophysical properties of isobutane are strongly needed for designing, operating, maintaining, or retrofitting purposes of technical equipment and are of great importance both in process simulations and in computational fluid dynamics. Basically, data accurately measured by means of high-precision experimental equipment form the basis for a state-of-the-art equation of state[1] and for a reliable reference viscosity surface correlation.[2]

The measuring apparatus used for the simultaneous determination of viscosity and density was designed by Seibt and a detailed description was given in his thesis.[3] The incorporated viscometer is based on the vibrating-wire technique using the know-how and operating experience obtained in measurements on gaseous fluids by Wilhelm et al.[4,5] Accordingly, a prerequisite for the evaluation of the viscosity measurements with the respective working equation is that the fluid density is established with an uncertainty as low as possible. In principle, both viscosity and density could be derived from the parameters of the measured oscillation curves of the vibrating wire, but the density can only be inferred with a considerably large uncertainty. Therefore, observed data for temperature and pressure are often utilized to calculate the density by means of an accurate equation of state. Unfortunately, the uncertainties of the measured temperatures and pressures do not only lead to an uncertainty in the density but also to a distinctly increased uncertainty of the resulting viscosity values. Consequently, Seibt complemented the viscometer by an accurate single-sinker densimeter to reduce this impact, in particular in the near-critical region. The experimental equipment was also communicated by Seibt et al.[6] in a report of viscosity and density measurements on helium and nitrogen which were used for a performance test of the apparatus. Then, it was concluded that, apart from the low-density region, the standard uncertainty in the density measured with the single-sinker method is

Correspondence concerning this article should be addressed to E. Vogel at eckhard.vogel@uni-rostock.de.

estimated to amount to 0.1%, so that the standard uncertainty in the viscosity could reach 0.3%. Note the uncertainties given for the measurements of this report represent standard uncertainties.

Recently, Seibt et al.[7] published the results of density and viscosity measurements on ethane and propane. In addition, Herrmann et al.[8] are preparing a report with new data of the density and viscosity for normal butane determined with the measuring apparatus under discussion, too. In this article, further simultaneous density and viscosity measurements on isobutane are submitted to extend the data base for the thermophysical properties of this fluid.

Experimental Section

Vibrating-wire viscometer

Only basic essentials of the design of the vibrating-wire viscometer operating in the transient mode are reviewed, as Seibt et al.[3,6] have already given the details. The wire made of Chromel® with an appropriately smooth surface has a length of 90 mm and a nominal diameter of 25 μm and is symmetrically assembled in a magnetic field. Hence all even and the third harmonic oscillation modes are practically prevented. The cobalt-samarium magnets are encased in magnetic stainless steel to guard them from corrosion and to prevent that the porous magnets absorb gas molecules. Three vibrating-wire viscometers are grouped circumferentially on the closure head of the measuring cell. The lower end of each wire is clamped between glass-ceramic blocks arranged at the end of a rotatable lever support which is implemented using two ruby bearings. The lever support prevents, particularly *in vacuo*, from a superimposed precession movement that could occur in the case of a freely suspended weight used in a former version of the viscometer. In addition, this arrangement warrants that the direction of the oscillation is perpendicular to the magnetic field.

A sinusoidal voltage pulse with a frequency close to the resonant frequency of the wire is applied to start the oscillation of the wire, then vibrating in its first mode. The initiated oscillation is recorded by amplifying the induced voltage and detecting it as a function of time. A run consists of hundred oscillations whose curves are measured and averaged to improve the signal-to-noise ratio. The logarithmic decrement Δ and the frequency ω of the oscillation are inferred by means of a nonlinear regression algorithm. As both the density and the radius of the wire are unproved, its density was supposed to be known, while the radius was determined by calibration. For that purpose, a value for the zero-density viscosity coefficient of helium deduced by Bich et al.[9] from an *ab initio* potential on the basis of the kinetic theory of dilute gases was used: $\eta_{0,^4\mathrm{He},293.15\mathrm{K}} = 19.600\ \mu\mathrm{Pas}$ with a standard uncertainty of 0.02%. The working equations to perform the calibration and to derive the viscosity η from the measurements can be found in Ref. 6.

Single-sinker densimeter

A single-sinker measuring device operating in the range of $1 \le \rho/\mathrm{kg\,m^{-3}} \le 2000$ was applied for measuring the density. It is based on the buoyancy principle, was developed at the Ruhr-Universität Bochum, and further improved by Klimeck et al.[10] An electronically controlled magnetic suspension coupling[11,12] enables the contactless transmission of the forces on the sinker within the pressure-tight measuring cell to a calibrated microbalance arranged above the thermostat under ambient conditions. An important issue for the design of the equipment was to guarantee that the magnetic fields of the vibrating-wire viscometer and of the suspension coupling do not interact. This was achieved by choosing a comparably large distance between the permanent magnet of the suspension coupling and the sinker which is placed in the midst of the three vibrating-wire viscometers. Whereas in the case of helium,[6] the density results were distinctly influenced by absorption processes on quartz glass selected as the sinker material for this previous investigation, the measurements on isobutane in this article using a silicon sinker do not suffer from such problems.

Temperature and pressure measurements

The temperature T was measured with a 25 Ω platinum resistance thermometer in conjunction with a precise resistance measuring bridge. The uncertainty of the temperature measurement amounts to 19 mK between 235 and 505 K, including the uncertainties of the thermometer (18 mK) as well as of the measuring bridge and of the control accuracy of the thermostat (each 2 mK). The temperature of the measuring cell is regulated utilizing a custom-built oil-filled double-wall thermostat with a vacuum vessel for its insulation. The outer stage of this two-stage thermostat is controlled by means of an oil thermostat within ±(10 to 50) mK, whereas its inner stage is governed by a heating tape regulated by a precise temperature controller within ±10 mK. In the end, the total uncertainty for the temperature is estimated to be $\Delta T/T \le 0.01\%$.

Four precise absolute transmitters with ranges of (41.4, 13.8, 2.76, and 0.689) MPa are applied for the measurement of the pressure p. They are distinguished by uncertainties of 0.01% of full scale and of (0.03 to 0.05)% from reading. A high-precision differential pressure transducer separates the measuring fluid-filled system from a nitrogen-filled gas system, in which the transmitters are operated to secure them from the condensable measuring fluid. This transducer is qualified for indicating pressure differences of ±5 kPa. It was calibrated with an uncertainty of 0.04% from reading, adding ≤0.002% to the uncertainty for measurements at pressures $p > 0.15$ MPa.

Condensation of the measuring fluid takes place in the connecting tubes to the measuring cell in the case of measurements for supercritical isotherms, when the pressure is lower than the critical one but higher than the saturation pressure, as well as for subcritical isotherms, when the pressure is higher than the saturation pressure. The reason is that the tubes are at ambient temperature, whereas the measuring cell situated within the thermostat features a higher temperature. To allow for this condensation, a liquid-level indicator located in a definite position of the connecting tubes is utilized. The temperature of this indicator is adjusted to a certain saturation temperature so that the pressure in the measuring cell is simultaneously in accordance with it.[3] The uncertainty of the hydrostatic pressure corrections is assessed to be 0.001% of the measured pressure value. In summary, the total uncertainty for the pressure adds up to $\Delta p/p \le 0.05\%$.

Error analysis

Seibt et al.[6] demonstrated the performance of the combined viscometer-densimeter on the basis of measurements

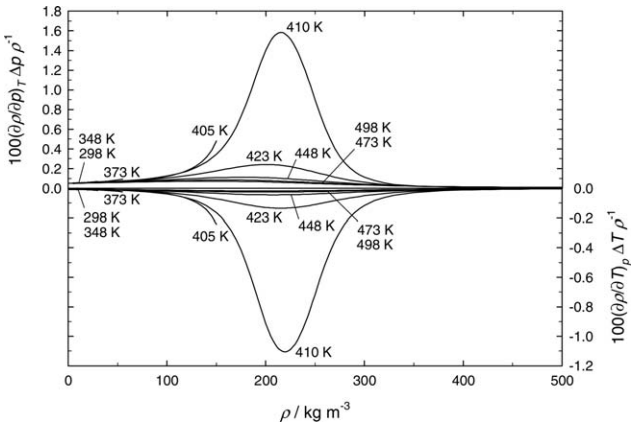

Figure 1. Allocation errors in pressure and temperature as a function of density ρ for isotherms of $p\rho T$ measurements on isobutane using the equation of state of Bücker and Wagner.[1]

on helium and nitrogen. In addition, they carried out a profound error analysis, which was extended to the somewhat more challenging situation of measurements on fluids like ethane and propane, particularly with regard to the near-critical region.[7]

Density. The total uncertainty of the $p\rho T$ data considers the uncertainty of the density $\Delta\rho/\rho$ as well as the allocation errors related to the uncertainties of the temperature and pressure measurements ΔT and Δp

$$\left(\frac{\Delta\rho}{\rho}\right)_{\text{tot}} = \left|\sqrt{\left(\frac{\Delta\rho}{\rho}\right)^2 + \left(\frac{\partial\rho}{\partial T}\right)_p^2 \frac{\Delta T^2}{\rho^2} + \left(\frac{\partial\rho}{\partial p}\right)_T^2 \frac{\Delta p^2}{\rho^2}}\right| \quad (1)$$

For the single-sinker apparatus, $\Delta\rho/\rho$ resulted as[6]

$$\frac{\Delta\rho}{\rho} \leq \left|0.0526\% + \frac{0.07\%}{\rho/(10\,\text{kg m}^{-3})}\right| \quad (2)$$

The allocation errors of T and p require the thermal expansion coefficient $(\partial\rho/\partial T)_p$ and the isothermal compressibility coefficient $(\partial\rho/\partial p)_T$ to be calculated from an available equation of state, sometimes only approximately. In principle, the impact of the uncertainties of ΔT and Δp is minor in wide thermodynamic regions due to its small values, as proven by Seibt et al.[6] for the measurements on helium and nitrogen, for which the total uncertainty of the density determination was $(\Delta\rho/\rho)_{\text{tot}} \leq 0.1\%$ for $\rho > 15$ kg m^{-3}. But near the critical region, a significant influence on the uncertainty of the density follows from the distinctly increased values for the partial derivatives $(\partial\rho/\partial T)_p$ and $(\partial\rho/\partial p)_T$, as illustrated by Seibt et al.[7] for ethane and propane.

For isobutane, the allocation errors were evaluated for the experimental data of temperature and pressure, taking into account the specified experimental uncertainties of pressure and temperature as well as $(\partial\rho/\partial T)_p$ and $(\partial\rho/\partial p)_T$ deduced from the equation of state by Bücker and Wagner.[1] Figure 1 indicates, for the near-critical isotherm at 410.15 K, maxima of -1.11% and of $+1.58\%$ for the allocation errors in the temperature and in the pressure, respectively. In conclusion, the maximum total uncertainty of the experimental $p\rho T$ data of this isotherm increases to $(\Delta\rho/\rho)_{\text{tot}} = 1.93\%$ (see Eq. 1).

Furthermore, the influence of impurities in the sample supplied by Gerling Holz & Co. (GHC) Handels GmbH, Hamburg, Germany, with a certified purity of $x_{\text{i-C}_4\text{H}_{10}} \leq 0.9999$ (isobutane 4.0), was investigated. On the one hand, an isobutane sample, characterized essentially by the product specification given by the supplier, but with the constraint that the sum of all mole fractions equals 1 (see caption of Figure 2), was examined. On the other hand, hypothetical isobutane samples, contaminated with the highest possible mole fraction of each individual impurity according to the declared product specification, were regarded. For all samples, densities were calculated using the equation of state for natural gases developed by Kunz and Wagner[13] and compared with values computed by means of the equation of state by Span and Wagner[14] for pure isobutane, which is preferred in this comparison, as Kunz and Wagner used the shorter equations of state developed by Span and Wagner in their project on natural gases. The deviations for the 410.15 K isotherm are illustrated in Figure 2 which makes obvious that the impurities due to higher alkanes result in systematic positive deviations, such as for *n*-pentane (+0.22%), whereas for lower alkanes like ethane and propane, negative deviations up to -0.42% and -0.17% occur. The maximum difference of -0.34% for the sample according to the product specification may be a conservative value, because the purity of the delivered samples is often better than that given in the product specification, as reported by Seibt et al.[7] for propane. Although the influence of impurities in the near-critical region is only one sixth of that caused by the allocation errors in pressure and temperature, the use of samples with a high purity is recommended.

Viscosity. The total uncertainty in the viscosity takes into account the uncertainty in the viscosity measurement itself as well as the allocation errors connected with the uncertainties of the temperature and density measurements

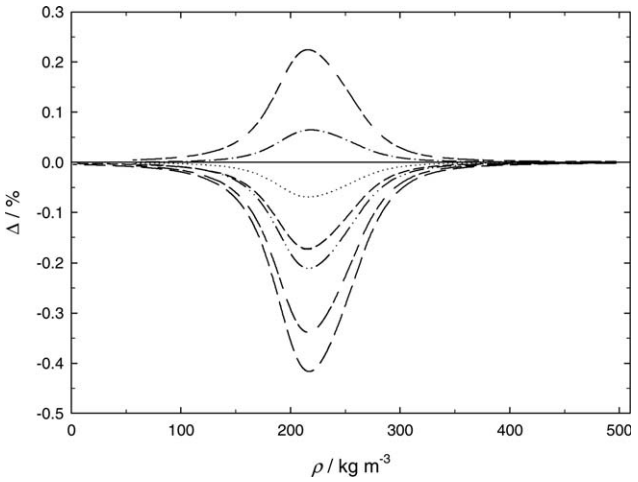

Figure 2. Comparison of calculated values $\rho_{\text{eos,cont}}$ for the density of contaminated samples of isobutane (equation of state of Kunz and Wagner[13]) at 410.15 K with calculated densities $\rho_{\text{eos,pure}}$ for pure isobutane (equation of state of Span and Wagner[14]), as a function of density ρ.

Deviations: $\Delta = 100(\rho_{\text{eos,cont}} - \rho_{\text{eos,pure}})/\rho_{\text{eos,pure}}$. — —, $x_{C_2H_6} = 90\times10^{-6}$; – –, $x_{C_3H_8} = 90\times10^{-6}$; – · –, $x_{n-C_4H_{10}} = 90\times10^{-6}$; – — –, $x_{i-C_5H_{12}} = 90\times10^{-6}$; – · · –, $x_{N_2} = 20\times10^{-6}$; · · · · · ·, $x_{O_2} = 5\times10^{-6}$; — – GHC isobutane 4.0 ($x_{N_2} = 15\times10^{-6}$, $x_{O_2} = 5\times10^{-6}$, $x_{H_2O} = 3\times10^{-6}$, $x_S = 0\times10^{-6}$, $x_{C_2H_6} = 22\times10^{-6}$, $x_{C_3H_8} = 25\times10^{-6}$, $x_{n-C_4H_{10}} = 30\times10^{-6}$).

Table 1. Experimental $\eta\rho pT$ Data for Isobutane at 298.15 K

T (K)	p (MPa)	$p_{298.15\mathrm{K},\rho_{\mathrm{exp}}}$ (MPa)	ρ_{exp} (kg m^{-3})	$\rho_{\mathrm{eos}(p,T)}$ (kg m^{-3})	η (μPa s)	$\eta_{298.15\ \mathrm{K}}$ (μPa s)
298.171	0.31049	0.31046	7.9659	7.9682	7.4213	7.4207
298.175	0.31108	0.31105	7.9835	7.9848	7.4214	7.4207
298.165	0.27731	0.27729	7.0386	7.0391	7.4298	7.4294
298.164	0.27731	0.27730	7.0401	7.0393	7.4283	7.4279
298.164	0.23974	0.23973	6.0112	6.0131	7.4385	7.4381
298.164	0.23974	0.23973	6.0112	6.0131	7.4375	7.4371
298.143	0.20152	0.20153	4.9929	4.9958	7.4448	7.4450
298.146	0.20152	0.20153	4.9929	4.9958	7.4470	7.4471
298.156	0.16339	0.16339	4.0022	4.0048	7.4551	7.4550
298.157	0.16339	0.16339	4.0022	4.0048	7.4542	7.4540
298.158	0.12390	0.12389	2.9992	3.0026	7.4654	7.4652
298.158	0.12390	0.12390	3.0000	3.0028	7.4647	7.4645
298.160	0.084022	0.084019	2.0123	2.0139	7.4730	7.4728
298.162	0.084025	0.084022	2.0131	2.0140	7.4718	7.4715

ΔT and $\Delta\rho$ and with the temperature and density dependencies of the viscosity

$$\left(\frac{\Delta\eta}{\eta}\right)_{\mathrm{tot}} = \left|\sqrt{\left(\frac{\Delta\eta}{\eta}\right)^2 + \left(\frac{\partial\eta}{\partial T}\right)_\rho^2 \frac{\Delta T^2}{\eta^2} + \left(\frac{\partial\eta}{\partial\rho}\right)_T^2 \frac{\Delta\rho^2}{\eta^2}}\right| \quad (3)$$

If the density required for the evaluation of the viscosity measurements is inferred from temperature and pressure measurements by means of an equation of state, the uncertainty of the viscosity determination is strongly increased, particularly with regard to the near-critical region, due to the enlargement of the allocation errors in temperature and pressure (see above). Fortunately, the simultaneous measurement of density and viscosity improves distinctly the state of affairs. Following Seibt et al.,[6] an analysis of multivariate functions was utilized to estimate the uncertainty in the viscosity measurement to be $\Delta\eta/\eta \leq (0.23 \text{ to } 0.28)\%$, if an uncertainty of $\Delta\rho/\rho \leq 0.1\%$ can be supposed for the density measurement.

The allocation errors were evaluated for the experimental data of temperature and density, taking into consideration the experimental uncertainties of temperature ($\Delta T/T \leq 0.01\%$) and of density ($\Delta\rho/\rho \leq 0.1\%$) as well as values for $(\partial\eta/\partial T)_\rho$ and $(\partial\eta/\partial\rho)_T$ deduced from the available viscosity surface correlation of isobutane by Vogel et al.[2] The influence of the allocation errors on the total uncertainty of the viscosity is only marginal following from comparably small values of $(\partial\eta/\partial T)_\rho$ and $(\partial\eta/\partial\rho)_T$, even in the near-critical region. One reason is that the contribution of the critical enhancement to the viscosity is small in the considered region. It comes only up to about +1% for the critical density, if the temperature is 1% higher than the critical one. In addition, the viscosity surface correlation of Vogel et al. does not include a contribution for the critical enhancement at all. In conclusion, the analysis results in a maximum total uncertainty $(\Delta\eta/\eta)_{\mathrm{tot}} = (0.25 \text{ to } 0.3)\%$ for the experimental $\eta\rho T$ data (Eq. 3), a little larger than the uncertainty in the viscosity measurement itself. Nevertheless, the uncertainty in the viscosity could still be increased in the near-critical region due to experimental difficulties.

Measurements and Results

Prior to each isothermal series of measurements, a determination of the logarithmic decrement Δ_0 of the wire oscillation and of the sinker mass $m_{\mathrm{s,vac}}$ *in vacuo* is undertaken. The series is started by filling the measuring apparatus with the fluid up to the highest pressure, at which the first experimental point is performed. The further points of the measuring program for each isothermal series are realized after reduction of the pressure by a discharge of the fluid and after attainment of the thermodynamic equilibrium. The time to accomplish equilibrium takes about several hours at the highest densities as well as in the near-critical region, whereas it reduces to about half an hour at low densities. A measuring point incorporates the determination of the logarithmic decrement Δ and of the frequency ω, evaluating runs, each with a hundred oscillations but started at different initial amplitudes, as well as three or more weighings of the sinker mass $m_{\mathrm{s,fluid.}}$ Measurements of temperature T and pressure p are simultaneously performed. A repeated determination of the logarithmic decrement and of the sinker mass *in vacuo* concludes each series of measurements. Further details of the measuring procedure have already been described by Seibt et al.[6]

Unfortunately, the individual points were not exactly carried out at the nominal temperature of an isotherm T_{nom}, but could be held within small deviations. The value ρ_{exp}, directly measured with the single-sinker densimeter at the temperature T and pressure p of the experimental point, corresponds to the density valid for the isotherm. Thus, the experimental viscosity value η was evaluated at T and p applying ρ_{exp}. In a next step, the viscosity data were adjusted to the nominal temperature so that $\eta_{T_{\mathrm{nom}}}$ values were obtained. For that purpose, a Taylor series expansion restricted to the first power in temperature was utilized. The temperature coefficient $(\partial\eta/\partial T)_\rho$ needed for the Taylor series expansion was derived from a double power-series expansion, which was fitted as a function of the reciprocal reduced temperature and as a function of the reduced density to the experimentally determined viscosities η. It has to be noted that the $(\partial\eta/\partial T)_\rho$ values determined in this manner are in accordance with $(\partial\eta/\partial T)_{\rho=0}$ values derived from reevaluated experimental low-density viscosity data by Küchenmeister and Vogel[15] which were extrapolated to the limit of zero density. In the end, the pressure at the nominal temperature, denoted $p_{T_{\mathrm{nom}},\rho_{\mathrm{exp}}}$, is another one as the pressure p at the temperature T, hence its value was recalculated for the experimental density ρ_{exp} using the equation of state by Bücker and Wagner.[1] In addition, density values according to the mentioned equation of state, $\rho_{\mathrm{eos}(p,T)}$, were computed for the measured data of the pressure p and

Table 2. Experimental $\eta\rho pT$ Data for Isobutane at 348.15 K

T (K)	p (MPa)	$p_{348.15\text{K},\rho_{exp}}$ (MPa)	ρ_{exp} (kg m^{-3})	$\rho_{eos(p,T)}$ (kg m^{-3})	η (μPa s)	$\eta_{348.15\ \text{K}}$ (μPa s)
348.175	1.1239	1.1237	28.714	28.717	8.8150	8.8143
348.178	1.1239	1.1237	28.712	28.717	8.8142	8.8134
348.153	1.0216	1.0216	25.318	25.316	8.7758	8.7757
348.151	1.0218	1.0218	25.321	25.322	8.7735	8.7735
348.150	0.76049	0.76049	17.626	17.618	8.7104	8.7104
348.166	0.76156	0.76151	17.652	17.646	8.7082	8.7078
348.169	0.69080	0.69075	15.757	15.751	8.6941	8.6936
348.166	0.69146	0.69141	15.772	15.768	8.6964	8.6960
348.153	0.62103	0.62102	13.954	13.948	8.6836	8.6835
348.153	0.62134	0.62133	13.954	13.956	8.6825	8.6824
348.157	0.53158	0.53157	11.726	11.720	8.6722	8.6720
348.158	0.53171	0.53169	11.730	11.723	8.6737	8.6735
348.166	0.45157	0.45154	9.8022	9.7997	8.6659	8.6655
348.166	0.45171	0.45169	9.8052	9.8031	8.6661	8.6657
348.169	0.36974	0.36972	7.9049	7.9012	8.6599	8.6595
348.165	0.37623	0.37621	8.0531	8.0496	8.6555	8.6551
348.126	0.28311	0.28313	5.9573	5.9571	8.6557	8.6562
348.137	0.28315	0.28316	5.9566	5.9577	8.6578	8.6581
348.170	0.19901	0.19900	4.1212	4.1266	8.6590	8.6585
348.166	0.19903	0.19902	4.1212	4.1269	8.6598	8.6594
348.168	0.098213	0.098208	2.0010	2.0028	8.6663	8.6659
348.168	0.098221	0.098216	2.0002	2.0030	8.6669	8.6665
348.144	0.061051	0.061052	1.2368	1.2377	8.6656	8.6657
348.144	0.061046	0.061047	1.2360	1.2376	8.6656	8.6657

temperature T. All these data and values are listed for the nine isothermal series of measurements on isobutane in Tables 1–9. Note some experimental points at the lowest densities were affected by the slip effect, they are marked. In addition, it is to note that the viscosity data of the 498.15 K isotherm for densities $\rho < 40$ kg m^{-3} (apart from five data points) suffered from a superposition by an additional precession movement; they are marked in Table 9. The viscosity data influenced by slip or by precession movement should be excluded from any use for viscosity correlations.

As already mentioned above, a sample isobutane 4.0 with a certified purity of $x_{\text{i-C}_4\text{H}_{10}} \leq 0.9999$ was used for the measurements. According to the product specification the impurities consist of $x_{N_2} \leq 20\times10^{-6}, x_{O_2} \leq 5\times10^{-6}, x_{H_2O} \leq 3\times10^{-6}, x_S \leq 1\times10^{-6}, x_{C_nH_m} \leq 90\times10^{-6}$. Four isotherms were recorded at subcritical temperatures (298.15, 348.15, 373.15, and 405.15 K) and five at supercritical ones (410.15, 423.15, 448.15, 473.15, and 498.15 K). The subcritical isotherms were performed up to about 93% of the saturated vapor pressure, whereas the supercritical isotherms were conducted up to 30 MPa. It is noteworthy that the first supercritical isotherm is only 2.34 K away from the critical temperature $T_c = 407.81$ K.

Evaluation of Data

Density

The results of the density measurements on isobutane are compared with values calculated for the equation of state of Bücker and Wagner.[1] This equation is valid from the triple-point temperature ($T_{tr,\text{i-C}_4\text{H}_{10}} = 113.73$ K) to 575 K and up to

Table 3. Experimental $\eta\rho pT$ Data for Isobutane at 373.15 K

T (K)	p (MPa)	$p_{373.15\text{K},\rho_{exp}}$ (MPa)	ρ_{exp} (kg m^{-3})	$\rho_{eos(p,T)}$ (kg m^{-3})	η (μPa s)	$\eta_{373.15\ \text{K}}$ (μPa s)
373.109	1.8177	1.8181	48.549	48.555	9.8648	9.8659
373.109	1.8183	1.8187	48.560	48.579	9.8663	9.8674
372.991	1.6054	1.6066	40.137	40.153	9.6850	9.6894
373.001	1.6057	1.6069	40.149	40.162	9.6933	9.6974
373.156	1.2879	1.2879	29.734	29.735	9.5110	9.5108
373.169	1.2878	1.2877	29.728	29.730	9.5135	9.5130
373.157	0.92838	0.92835	19.953	19.956	9.3783	9.3781
373.158	0.92837	0.92834	19.952	19.956	9.3741	9.3739
373.164	0.75749	0.75745	15.802	15.810	9.3309	9.3306
373.166	0.75728	0.75724	15.805	15.805	9.3320	9.3316
373.159	0.58588	0.58586	11.902	11.898	9.2985	9.2983
373.159	0.58617	0.58615	11.908	11.904	9.2999	9.2997
373.150	0.49058	0.49058	9.8283	9.8208	9.2879	9.2879
373.149	0.49093	0.49093	9.8329	9.8284	9.2849	9.2849
373.149	0.40205	0.40205	7.9468	7.9457	9.2728	9.2728
373.149	0.40129	0.40129	7.9300	7.9298	9.2744	9.2744
373.151	0.25690	0.25690	4.9762	4.9755	9.2640	9.2640
373.151	0.25692	0.25692	4.9769	4.9759	9.2615	9.2615
373.154	0.15656	0.15655	2.9909	2.9919	9.2556	9.2555
373.156	0.15657	0.15656	2.9924	2.9921	9.2550	9.2549
373.156	0.063643	0.063641	1.2018	1.2018	9.2538	9.2537
373.160	0.063649	0.063647	1.2026	1.2019	9.2511	9.2509

Table 4. Experimental $\eta\rho pT$ Data for Isobutane at 405.15 K

T (K)	p (MPa)	$p_{405.15\text{K},\rho_{exp}}$ (MPa)	ρ_{exp} (kg m^{-3})	$\rho_{eos(p,T)}$ (kg m^{-3})	η (μPa s)	$\eta_{405.15\ \text{K}}$ (μPa s)
405.152	3.0939	3.0939	93.694	93.772	12.442	12.442
405.147	3.0928	3.0929	93.686	93.697	12.449	12.449
405.142	3.0936	3.0938	93.754	93.766	12.443	12.443
405.144	3.0398	3.0399	89.917	89.915	12.271	12.271
405.153	3.0396	3.0396	89.894	89.894	12.251	12.250
405.169	3.0394	3.0390	89.852	89.856	12.274	12.274
405.109	2.8800	2.8807	80.091	80.093	11.852	11.853
405.112	2.8800	2.8807	80.091	80.095	11.850	11.851
405.162	2.6854	2.6852	70.133	70.158	11.473	11.472
405.172	2.6854	2.6850	70.122	70.151	11.473	11.472
405.138	2.4146	2.4148	58.801	58.812	11.079	11.079
405.141	2.4128	2.4129	58.726	58.741	11.077	11.077
405.139	2.1651	2.1652	49.944	49.952	10.818	10.819
405.142	2.1651	2.1652	49.944	49.951	10.812	10.812
405.143	1.8253	1.8254	39.553	39.551	10.553	10.554
405.153	1.8246	1.8246	39.532	39.530	10.543	10.542
405.158	1.8242	1.8241	39.517	39.516	10.540	10.540
405.164	1.4595	1.4594	29.860	29.855	10.357	10.356
405.170	1.4593	1.4592	29.853	29.851	10.333	10.333
405.175	1.4592	1.4591	29.849	29.846	10.352	10.351
405.179	1.0330	1.0329	19.945	19.946	10.182	10.181
405.175	1.0330	1.0329	19.944	19.946	10.173	10.172
405.111	0.93264	0.93275	17.789	17.789	10.133	10.134
405.136	0.93193	0.93197	17.773	17.773	10.146	10.146
405.138	0.93203	0.93207	17.777	17.775	10.139	10.139
405.138	0.85252	0.85255	16.106	16.103	10.102	10.102
405.139	0.85269	0.85271	16.107	16.107	10.121	10.121
405.144	0.85334	0.85335	16.122	16.120	10.131	10.131
405.173	0.73720	0.73715	13.737	13.737	10.090	10.090
405.173	0.73738	0.73733	13.743	13.741	10.100	10.099
405.093	0.64754	0.64765	11.954	11.947	10.054	10.056
405.096	0.64768	0.64777	11.956	11.950	10.050	10.051
405.154	0.54571	0.54571	9.9567	9.9537	10.055	10.055
405.162	0.54589	0.54587	9.9613	9.9568	10.041	10.040
405.162	0.54609	0.54607	9.9651	9.9607	10.034	10.034
405.164	0.43960	0.43959	7.9302	7.9271	10.028	10.028
405.160	0.44235	0.44234	7.9813	7.9790	10.035	10.035
405.160	0.30414	0.30414	5.4101	5.4076	10.019	10.019
405.164	0.30551	0.30549	5.4368	5.4325	10.011	10.010
405.175	0.22531	0.22530	3.9757	3.9739	10.001	10.001
405.178	0.22532	0.22530	3.9757	3.9740	9.9872	9.9865
405.182	0.22534	0.22532	3.9780	3.9743	9.9947	9.9940
405.136	0.11575	0.11575	2.0209	2.0197	9.9901	9.9904
405.138	0.11576	0.11576	2.0194	2.0198	10.019	10.020
405.139	0.11577	0.11578	2.0202	2.0201	10.009	10.009
405.131	0.061118	0.061121	1.0619	1.0608	*9.9644**	*9.9648**
405.137	0.061123	0.061125	1.0603	1.0609	10.005	10.006
405.210	0.061200	0.061191	1.0626	1.0620	10.004	10.003

*Influenced by slip.

pressures of 35 MPa. The authors state the uncertainty in the density to be 0.02% (coverage factor $k = 2$) for temperatures up to 340 K and pressures up to 12 MPa based primarily on measurements of Glos et al.[16,17] at the Ruhr-Universität Bochum with a two-sinker densimeter. The further gaseous subcritical region studied in this work features an uncertainty of (0.1 to 0.15)%. The remaining thermodynamic range covered at supercritical temperatures is characterized by uncertainties of (0.1 to 0.5)% ($T \leq 420$ K), (0.1 to 0.15)% ($420 < T/\text{K} \leq 450$), and 0.4% ($450 < T/\text{K} \leq 600$, adequately extrapolated) as well as by an uncertainty in pressure of 0.5% for the extended critical region. These uncertainties correspond to those of the reliable experimental datasets considered by Bücker and Wagner when developing the equation of state.

Figure 3 represents the deviations in density of the experimental data of this article from the values calculated for the equation of state of Bücker and Wagner[1] using the measured temperatures and pressures. The figure illustrates additionally, for the isotherm 410.15 K, the uncertainty of the density measurement and the uncertainty of the equation of state for the range of supercritical pressures (0.5%). For the isotherm 298.15 K, the deviations are at most −0.11% at $\rho = 3.00$ kg m^{-3}, lower than the uncertainty of the single-sinker densimeter but distinctly above the uncertainty of the equation of state in this region (0.02%). Apart from four measuring points at 348.15 K (up to −0.14% at $\rho \leq 4.12$ kg m^{-3}), the density data for the isotherms 348.15, 373.15, and 405.15 K are described within the uncertainty of the equation of state for this range (0.1%). The figure reveals maximum differences up to −3.72% for the near-critical isotherm at 410.15 K in the range $169 \leq \rho/\text{kg m}^{-3} \leq 255$. As already stated, the maximum total uncertainty of experimental $p\rho T$ data could amount to 1.93% or even up to 2.27% (including the possible effect of impurities) for this isotherm. The density data for the isotherms 423.15 and 448.15 K

Table 5. Experimental $\eta\rho pT$ Data for Isobutane at 410.15 K

T (K)	p (MPa)	$p_{410.15K,\rho_{exp}}$ (MPa)	ρ_{exp} (kg m^{-3})	$\rho_{eos(p,T)}$ (kg m^{-3})	η (μPa s)	$\eta_{410.15\ K}$ (μPa s)
410.168	30.138	30.138	496.70	496.86	100.79	100.78
410.166	30.141	30.142	496.71	496.87	100.57	100.57
410.153	30.164	30.170	496.77	496.93	100.74	100.74
410.126	23.443	23.458	479.97	480.01	90.078	90.079
410.127	23.446	23.461	479.99	480.02	90.263	90.264
410.132	23.459	23.472	480.01	480.05	90.269	90.269
410.135	17.398	17.408	460.28	460.18	79.800	79.800
410.137	17.398	17.408	460.28	460.18	79.732	79.732
410.143	17.399	17.407	460.28	460.17	79.809	79.809
410.145	12.816	12.822	439.89	439.69	70.557	70.557
410.167	9.6971	9.6974	420.49	420.21	62.962	62.961
410.173	9.6989	9.6978	420.49	420.21	63.070	63.069
410.180	9.6997	9.6969	420.48	420.20	62.949	62.948
410.151	7.5667	7.5701	401.73	401.41	56.700	56.700
410.142	7.5668	7.5720	401.75	401.43	56.690	56.690
410.159	5.9521	5.9537	380.46	380.08	50.451	50.450
410.147	5.9503	5.9539	380.46	380.08	50.381	50.381
410.137	5.9514	5.9568	380.47	380.13	50.413	50.413
410.149	5.0025	5.0053	360.73	360.26	45.284	45.284
410.151	5.0038	5.0063	360.77	360.29	45.321	45.321
410.150	4.4252	4.4275	341.05	340.43	40.898	40.898
410.163	4.4269	4.4275	341.04	340.43	40.912	40.911
410.168	4.0940	4.0940	320.95	320.31	36.979	36.978
410.167	4.0939	4.0940	320.94	320.30	36.923	36.922
410.150	3.9219	3.9236	301.25	300.81	33.383	33.383
410.142	3.9212	3.9236	301.27	300.82	33.428	33.428
410.139	3.9211	3.9238	301.29	300.84	33.406	33.406
410.176	3.8425	3.8419	281.67	281.77	30.310	30.309
410.178	3.8430	3.8422	281.68	281.89	30.334	30.334
410.152	3.7959	3.7970	254.93	256.81	26.702*	26.702*
410.157	3.7963	3.7971	254.97	256.91	26.749*	26.749*
410.159	3.7965	3.7971	255.00	256.90	26.727*	26.727*
410.162	3.7831	3.7835	235.72	240.59	24.413*	24.413*
410.172	3.7835	3.7833	235.75	240.29	24.400*	24.400*
410.170	3.7835	3.7833	235.74	240.41	24.358*	24.358*
410.115	3.7782	3.7817	231.79	237.84	23.945*	23.945*
410.116	3.7782	3.7816	231.75	237.79	23.934*	23.934*
410.144	3.7764	3.7779	224.05	231.66	23.080*	23.080*
410.149	3.7767	3.7779	224.06	231.70	23.055*	23.055*
410.153	3.7751	3.7760	220.85	228.46	22.672*	22.671*
410.161	3.7756	3.7761	220.86	228.55	22.720*	22.720*
410.163	3.7756	3.7759	220.80	228.32	22.720*	22.719*
410.157	3.7719	3.7726	214.30	222.31	21.963*	21.963*
410.160	3.7721	3.7726	214.33	222.40	21.989*	21.989*
410.162	3.7722	3.7726	214.33	222.32	21.945*	21.945*
410.183	3.7700	3.7691	208.12	216.08	21.277*	21.276*
410.197	3.7709	3.7692	208.14	216.12	21.243*	21.242*
410.207	3.7713	3.7690	208.13	215.84	21.277*	21.276*
410.141	3.7646	3.7661	202.92	210.76	20.731*	20.731*
410.149	3.7650	3.7661	202.97	210.65	20.766*	20.766*
410.144	3.7645	3.7659	202.97	210.41	20.690*	20.690*
410.146	3.7618	3.7631	198.88	205.53	20.281*	20.281*
410.147	3.7619	3.7631	198.90	205.61	20.312*	20.312*
410.142	3.7615	3.7630	198.88	205.41	20.267*	20.267*
410.147	3.7593	3.7605	195.92	201.51	19.977*	19.977*
410.153	3.7598	3.7606	195.94	201.66	20.005*	20.005*
410.171	3.7608	3.7606	195.95	201.69	19.985*	19.984*
410.153	3.7515	3.7522	186.84	190.40	19.125*	19.125*
410.153	3.7515	3.7522	186.86	190.40	19.096*	19.096*
410.157	3.7517	3.7523	186.88	190.43	19.090*	19.090*
410.131	3.7386	3.7404	177.07	179.02	18.157	18.158
410.127	3.7384	3.7405	177.08	179.09	18.156	18.156
410.165	3.7266	3.7267	168.98	169.89	17.434	17.433
410.166	3.7266	3.7267	168.98	169.89	17.449	17.449
410.149	3.7062	3.7070	160.43	160.51	16.745	16.745
410.153	3.7065	3.7071	160.41	160.57	16.753	16.753
410.151	3.6708	3.6715	148.83	148.88	15.870	15.870
410.155	3.6711	3.6716	148.88	148.91	15.868	15.868
410.147	3.6316	3.6323	139.80	139.74	15.220	15.220
410.145	3.6314	3.6322	139.78	139.72	15.224	15.225
410.149	3.4984	3.4990	119.53	119.52	13.949	13.949
410.153	3.4984	3.4989	119.52	119.51	13.951	13.951
410.142	3.2896	3.2902	100.00	100.06	12.888	12.888

TABLE 5. *Continued*

T (K)	p (MPa)	$p_{410.15K,\rho_{exp}}$ (MPa)	ρ_{exp} (kg m^{-3})	$\rho_{eos(\rho,T)}$ (kg m^{-3})	η (μPa s)	$\eta_{410.15\ K}$ (μPa s)
410.152	3.2899	3.2903	100.01	100.06	12.903	12.903
410.153	3.2900	3.2904	100.01	100.07	12.889	12.889
410.160	3.1288	3.1290	89.064	89.110	12.381	12.381
410.170	3.1293	3.1292	89.082	89.125	12.372	12.371
410.183	2.9535	2.9532	79.264	79.313	11.963	11.962
410.190	2.9537	2.9533	79.269	79.317	11.964	11.962
410.110	2.7403	2.7411	69.351	69.382	11.597	11.598
410.115	2.7402	2.7410	69.349	69.378	11.590	11.591
410.155	2.4898	2.4900	59.403	59.410	11.255	11.255
410.160	2.4905	2.4906	59.426	59.432	11.247	11.247
410.175	2.2173	2.2172	50.082	50.082	10.966	10.966
410.174	2.2179	2.2178	50.101	50.101	10.970	10.969
410.204	1.8713	1.8711	39.820	39.819	10.692	10.691
410.178	1.8703	1.8703	39.799	39.796	10.691	10.690
410.123	1.4584	1.4586	29.218	29.214	10.463	10.463
410.127	1.4591	1.4593	29.235	29.230	10.462	10.463
410.142	1.0452	1.0453	19.866	19.863	10.299	10.299
410.130	1.0454	1.0455	19.869	19.867	10.306	10.307
410.130	0.95307	0.95317	17.917	17.917	10.266	10.267
410.129	0.95308	0.95319	17.916	17.917	10.262	10.262
410.168	0.84797	0.84797	15.748	15.748	10.244	10.243
410.167	0.84778	0.84778	15.748	15.745	10.245	10.245
410.199	0.73603	0.73597	13.500	13.500	10.229	10.228
410.197	0.73484	0.73478	13.477	13.476	10.225	10.223
410.137	0.64414	0.64420	11.706	11.700	10.187	10.188
410.132	0.64359	0.64366	11.695	11.689	10.209	10.209
410.143	0.47460	0.47463	8.4726	8.4688	10.155	10.155
410.141	0.47451	0.47455	8.4711	8.4673	10.155	10.155
410.118	0.33985	0.33990	5.9869	5.9832	10.150	10.151
410.126	0.34067	0.34070	6.0014	5.9979	10.152	10.153
410.169	0.14663	0.14663	2.5354	2.5333	10.136	10.136
410.171	0.14746	0.14746	2.5492	2.5478	10.127	10.127
410.137	0.077804	0.077810	1.3361	1.3357	10.130	10.130
410.136	0.078308	0.078314	1.3445	1.3444	10.120	10.120

*Influenced by the near-critical region.

show the greatest deviations around the value of the critical density, too. But, these deviations come only up to -0.10% and $+0.15\%$, clearly within the uncertainty of the equation of state. The experimental data of the two highest isotherms (473.15 and 498.15 K) are distinguished by deviations, considerably lower than the uncertainty of the equation of state (0.4%), except for two points at 473.15 K and at the lowest density. In summary, the experimental density data of isobutane for the near-critical isotherm at 410.15 K reveal deviations from values for the reference equation of state of Bücker and Wagner,[1] distinctly higher than the differences in the case of the near-critical isotherms of ethane and propane,[6] for which the experimental data were contrasted with the reference equations of state of Bücker and Wagner[18] and of Lemmon et al.,[19] respectively. Further, the deviations for the near-critical isotherm of isobutane are twice as large as the uncertainty of the single-sinker densimeter, whereas the analogous differences for ethane and propane are actually a little lower than the experimental uncertainty estimated for the respective near-critical isotherms, as reported by Seibt et al.[6]

The large deviations of the experimental density data at 410.15 K from values calculated according to the reference equation of state of Bücker and Wagner[1] provoked a further comparison with other equations of state. Figure 4 illustrates once again at 410.15 K the deviations from the equation of state of Younglove and Ely[20] as well as from the fundamental equations of state of Miyamoto and Watanabe,[21] of Span and Wagner,[14] and naturally of Bücker and Wagner. For densities $\rho \leq 100\ \mathrm{kg\,m^{-3}}$ and $\rho \geq 321\ \mathrm{kg\,m^{-3}}$, the deviations for the four equations differ only a little and are within $\pm 0.75\%$. The maximum deviations occur next to the critical density $\rho_c = 225.5\ \mathrm{kg\,m^{-3}}$. Positive deviations result for the three older equations of state: $+4.43\%$ at $\rho = 255\ \mathrm{kg\,m^{-3}}$ for Younglove and Ely, $+7.29\%$ at $\rho = 236\ \mathrm{kg\,m^{-3}}$ for Miyamoto and Watanabe, $+3.87\%$ at $\rho = 255\ \mathrm{kg\,m^{-3}}$ for Span and Wagner. These similar deviations of the experimental density data from the three equations of state lead to the conclusion that nearly analogous datasets with the same weighings were used to generate the equations. In contrast, negative deviations result for the reference equation of state of Bücker and Wagner (-3.72% at $\rho = 203\ \mathrm{kg\,m^{-3}}$ as maximum). This implies that a comparison with measured density data (see below) could be promising to find the reason for the different trend of the deviations and particularly for their large values. In addition, an uncertainty in density of 0.5% shown in the figure is certainly not representative for the equation of state of Bücker and Wagner, and it is also not for the other equations of state, at this temperature in the near-critical region. An estimation for the uncertainty in density, based on the uncertainty in pressure, could be made by the assumption that for simple hydrocarbons the relative error $\Delta\rho/\rho$ is several times larger than that of $\Delta p/p$. But, a value of 5% which would result from choosing 10 times the uncertainty in pressure is, even in the near-critical region, probably too high.

As argued, a comparison of specific experimental density data with density values calculated using the equation of state of Bücker and Wagner[1] could enable to recover the reason for the exceedingly large deviations in the near-critical

Table 6. Experimental $\eta\rho pT$ Data for Isobutane at 423.15 K

T (K)	p (MPa)	$p_{423.15K,\rho_{exp}}$ (MPa)	ρ_{exp} (kg m^{-3})	$\rho_{eos(p,T)}$ (kg m^{-3})	η (μPa s)	$\eta_{423.15\ K}$ (μPa s)
423.139	29.950	29.954	484.66	484.85	93.343	93.344
423.137	29.946	29.951	484.65	484.84	93.261	93.261
423.079	28.029	28.055	479.89	480.03	90.531	90.532
423.075	28.029	28.055	479.89	480.03	90.498	90.500
423.142	21.318	21.321	459.80	459.80	79.754	79.755
423.149	21.319	21.320	459.80	459.80	79.876	79.876
423.159	21.322	21.319	459.80	459.79	79.894	79.894
423.137	16.112	16.116	438.87	438.75	70.329	70.329
423.138	16.113	16.116	438.87	438.75	70.318	70.318
423.163	12.770	12.767	420.57	420.39	63.270	63.270
423.163	12.771	12.768	420.57	420.40	63.291	63.291
423.157	12.769	12.767	420.57	420.39	63.286	63.286
423.129	10.067	10.072	400.30	400.10	56.503	56.504
423.135	10.068	10.071	400.29	400.10	56.498	56.499
423.136	10.069	10.071	400.29	400.10	56.481	56.481
423.151	8.2301	8.2299	380.53	380.34	50.694	50.694
423.147	8.2292	8.2297	380.52	380.34	50.707	50.707
423.149	8.2293	8.2295	380.52	380.34	50.687	50.687
423.156	6.9617	6.9608	360.71	360.54	45.609	45.609
423.166	6.9629	6.9605	360.70	360.54	45.631	45.631
423.173	6.9636	6.9601	360.69	360.53	45.646	45.645
423.186	6.0917	6.0870	340.23	340.09	41.009	41.009
423.189	6.0920	6.0869	340.22	340.09	41.028	41.027
423.193	6.0921	6.0865	340.21	340.08	40.994	40.992
423.106	5.5564	5.5614	321.56	321.45	37.268	37.269
423.105	5.5563	5.5615	321.56	321.46	37.263	37.264
423.100	5.5559	5.5616	321.57	321.46	37.251	37.252
423.132	5.1538	5.1556	299.10	299.05	33.280	33.280
423.132	5.1538	5.1555	299.10	299.05	33.279	33.279
423.135	5.1541	5.1556	299.10	299.05	33.278	33.278
423.147	4.9536	4.9538	282.03	282.02	30.570	30.570
423.145	4.9535	4.9539	282.03	282.03	30.567	30.567
423.145	4.9533	4.9537	282.02	282.01	30.572	30.572
423.171	4.7799	4.7782	260.41	260.50	27.482	27.481
423.180	4.7806	4.7783	260.42	260.51	27.481	27.480
423.186	4.7810	4.7782	260.42	260.50	27.485	27.484
423.166	4.7148	4.7136	250.02	250.15	26.125	26.124
423.168	4.7150	4.7137	250.03	250.16	26.130	26.129
423.173	4.7154	4.7137	250.04	250.17	26.133	26.132
423.142	4.6505	4.6511	238.48	238.63	24.701	24.702
423.130	4.6497	4.6510	238.48	238.63	24.702	24.702
423.142	4.6004	4.6009	228.23	228.40	23.503	23.503
423.143	4.6005	4.6009	228.22	228.40	23.500	23.500
423.189	4.5618	4.5594	219.24	219.45	22.507	22.506
423.190	4.5619	4.5595	219.25	219.46	22.506	22.505
423.117	4.5148	4.5168	209.82	210.00	21.512	21.512
423.113	4.5146	4.5167	209.84	210.00	21.516	21.517
423.157	4.4728	4.4725	200.18	200.27	20.550	20.550
423.154	4.4727	4.4725	200.17	200.27	20.549	20.549
423.138	4.4228	4.4234	189.93	189.93	19.577	19.578
423.137	4.4228	4.4235	189.94	189.94	19.577	19.577
423.144	4.3690	4.3693	179.35	179.34	18.636	18.636
423.155	4.3696	4.3694	179.37	179.36	18.642	18.642
423.142	4.2532	4.2536	160.15	160.09	17.069	17.069
423.138	4.2531	4.2536	160.15	160.09	17.068	17.069
423.177	4.1000	4.0990	140.45	140.41	15.649	15.648
423.175	4.1001	4.0992	140.47	140.43	15.648	15.647
423.150	3.8692	3.8692	119.10	119.09	14.313	14.313
423.145	3.8691	3.8693	119.09	119.09	14.316	14.316
423.152	3.5528	3.5527	97.987	98.024	13.190	13.190
423.162	3.5530	3.5528	97.986	98.024	13.187	13.187
423.184	3.3903	3.3896	89.311	89.341	12.783	12.782
423.184	3.3901	3.3895	89.302	89.333	12.782	12.781
423.167	3.1694	3.1691	79.095	79.129	12.337	12.337
423.166	3.1697	3.1694	79.109	79.143	12.341	12.340
423.123	2.9275	2.9278	69.412	69.433	11.959	11.960
423.121	2.9277	2.9281	69.425	69.441	11.960	11.961
423.140	2.6195	2.6196	58.664	58.669	11.582	11.582
423.135	2.6195	2.6197	58.666	58.673	11.582	11.582
423.165	2.3045	2.3044	49.043	49.043	11.286	11.285
423.163	2.3043	2.3042	49.038	49.038	11.284	11.284
423.156	1.9570	1.9569	39.637	39.633	11.028	11.028
423.149	1.9577	1.9577	39.656	39.653	11.031	11.031

TABLE 6. *Continued*

T (K)	p (MPa)	$p_{423.15K,\rho_{exp}}$ (MPa)	ρ_{exp} (kg m^{-3})	$\rho_{eos(\rho,T)}$ (kg m^{-3})	η (μPa s)	$\eta_{423.15\ K}$ (μPa s)
423.158	1.7686	1.7686	34.955	34.950	10.914	10.914
423.151	1.7689	1.7689	34.960	34.958	10.916	10.916
423.149	1.7690	1.7690	34.964	34.960	10.916	10.916
423.144	1.5232	1.5232	29.216	29.213	10.789	10.789
423.137	1.5231	1.5232	29.216	29.213	10.791	10.791
423.176	1.3146	1.3145	24.616	24.616	10.699	10.698
423.185	1.3147	1.3145	24.618	24.617	10.702	10.701
423.206	1.0703	1.0701	19.518	19.519	10.611	10.610
423.215	1.0702	1.0700	19.517	19.518	10.612	10.611
423.124	0.96324	0.96332	17.378	17.380	10.577	10.578
423.119	0.96375	0.96383	17.389	17.390	10.576	10.577
423.130	0.87053	0.87058	15.574	15.561	10.547	10.547
423.128	0.87131	0.87136	15.574	15.576	10.548	10.549
423.120	0.75882	0.75888	13.410	13.417	10.523	10.524
423.124	0.96324	0.96332	17.378	17.380	10.577	10.578
423.119	0.96375	0.96383	17.389	17.390	10.576	10.577
423.130	0.87053	0.87058	15.574	15.561	10.547	10.547
423.128	0.87131	0.87136	15.574	15.576	10.548	10.549
423.120	0.75882	0.75888	13.410	13.417	10.523	10.524
423.124	0.75885	0.75891	13.415	13.417	10.522	10.522
423.125	0.67893	0.67897	11.913	11.912	10.503	10.503
423.123	0.67907	0.67912	11.916	11.915	10.503	10.503
423.142	0.58071	0.58073	10.096	10.095	10.483	10.484
423.150	0.58068	0.58068	10.094	10.094	10.483	10.483
423.180	0.45638	0.45634	7.8448	7.8425	10.463	10.462
423.189	0.45542	0.45537	7.8265	7.8252	10.461	10.460
423.150	0.35337	0.35337	6.0163	6.0170	10.438	10.438
423.144	0.35486	0.35486	6.0415	6.0433	10.441	10.441
423.169	0.23524	0.23523	3.9636	3.9642	10.426	10.425
423.170	0.23532	0.23530	3.9659	3.9654	10.425	10.424
423.188	0.12028	0.12027	2.0077	2.0070	10.408	10.407
423.188	0.12028	0.12027	2.0069	2.0070	10.409	10.408
423.138	0.059679	0.059681	0.99085	0.99084	10.398	10.399
423.152	0.059692	0.059692	0.99161	0.99103	*10.393**	*10.392**

*Influenced by slip.

region. For that purpose, Figure 5 represents the deviations of new experimental density data from the literature, measured after development of the reference equation of state and hence not considered by Bücker and Wagner, as well as of the density data of this work at temperatures between 405 and 410.15 K. Miyamoto et al.[22] carried out $p\rho T$ measurements for three subcritical isotherms (405, 406, and 407 K) in the liquid phase as well as for the saturated liquid on the saturation curve at the same temperatures. These measurements are characterized by an uncertainty of 0.08%. For all three isotherms in the density range $295 < \rho/\mathrm{kg\,m^{-3}} < 320$, the data do not deviate more than $\pm 0.5\%$ from the calculated values for the reference equation of state. Then, the deviations increase with decreasing density up to -2.46% at $\rho = 275\ \mathrm{kg\,m^{-3}}$. Similar differences appear for the saturated liquid, the largest with -3.18% at $\rho = 272\ \mathrm{kg\,m^{-3}}$ for 407 K. Masui et al.,[23] from the same working group, performed $p\rho T$ measurements between 405 and 410 K in the compressed gas phase and in the supercritical fluid. The results of this dataset, labeled below as the second one from this work, are regrettably distinguished by greater uncertainties at subcritical temperatures. Hence only data for the isotherm 410 K characterized by an uncertainty of $\Delta\rho/\rho = (0.3 \text{ to } 0.4)\%$ were selected to be represented in Figure 5. These data exhibit deviations from density values, calculated using the equation of state of Bücker and Wagner,[1] between -1.85% at $\rho = 265\ \mathrm{kg\,m^{-3}}$ and -7.14% at $\rho = 210\ \mathrm{kg\,m^{-3}}$. As the deviations of the new density data of Miyamoto et al. and of Masui et al. from the reference equation of state of Bücker and Wagner are similar in size as those of the measured densities of this work, it can be concluded that all these new data support the further improvement of the currently used reference equation of state.

With regard to the other equations of state discussed above, it is to indicate that the data of Masui et al.[23] at 410 K deviate from the equation of state of Miyamoto and Watanabe[21] up to $+4.28\%$, whereas they agree within $\pm 2.43\%$ and $\pm 1.71\%$ with the calculated density values resulting from the equations of state of Younglove and Ely[20] and of Span and Wagner,[14] respectively. A similarly graded series of deviations (-3.72 to $+7.29\%$) was discovered in the comparison of the measured density data of this work at 410.15 K with the four discussed equations of state as already demonstrated in Figure 4. Thus, this behavior should be due to different primary density datasets utilized within the scope of generating the respective equation of state.

In connection with the discussed uncertainties for the reference equation of state of Bücker and Wagner,[1] it has already been pointed that in the near-critical region the measured pressures should preferably be compared with pressures calculated using the different equations of state and the measured temperatures and densities. Thus, Figure 6 illustrates that, for the isotherm at 410.15 K, the deviations of the experimental data from the calculated pressures for the four aforementioned equations of state in the density range $\rho \leq 282\ \mathrm{kg\,m^{-3}}$ do not exceed $\pm 0.47\%$ and for densities $\rho \leq 380\ \mathrm{kg\,m^{-3}}$ do not go beyond -0.61%. The deviations for the equation of state of Younglove und Ely[20]increase subsequently with increasing density up to -0.93% at $\rho \leq 480\ \mathrm{kg\,m^{-3}}$ and decrease again at the

Table 7. Experimental $\eta\rho pT$ Data for Isobutane at 448.15 K

T (K)	p (MPa)	$p_{448.15K,\rho_{exp}}$ (MPa)	ρ_{exp} (kg m^{-3})	$\rho_{eos(p,T)}$ (kg m^{-3})	η (μPa s)	$\eta_{448.15\ K}$ (μPa s)
448.153	29.956	29.955	462.29	462.48	81.724	81.724
448.145	29.956	29.958	462.29	462.49	81.886	81.886
448.148	29.962	29.963	462.30	462.50	81.746	81.746
448.135	28.940	28.945	459.37	459.54	80.496	80.496
448.143	28.943	28.945	459.37	459.54	80.331	80.331
448.152	28.946	28.946	459.37	459.54	80.326	80.326
448.102	23.082	23.095	439.78	439.82	71.502	71.503
448.094	23.087	23.102	439.81	439.85	71.547	71.549
448.092	23.093	23.109	439.83	439.87	71.492	71.494
448.139	18.611	18.614	420.11	420.06	63.851	63.851
448.140	18.614	18.616	420.12	420.07	63.886	63.886
448.139	18.615	18.617	420.12	420.08	63.850	63.850
448.135	15.185	15.188	400.08	400.01	57.135	57.135
448.133	15.185	15.188	400.08	400.01	57.082	57.083
448.135	15.185	15.188	400.08	400.01	57.138	57.138
448.151	12.633	12.632	379.89	379.86	51.244	51.244
448.162	12.634	12.632	379.89	379.85	51.259	51.259
448.145	10.759	10.760	359.68	359.71	46.100	46.100
448.139	10.759	10.761	359.70	359.73	46.116	46.116
448.123	9.4399	9.4436	340.29	340.37	41.748	41.749
448.131	9.4406	9.4432	340.29	340.36	41.706	41.707
448.136	9.4421	9.4440	340.30	340.38	41.711	41.711
448.127	8.4440	8.4467	320.25	320.35	37.682	37.683
448.132	8.4443	8.4464	320.24	320.34	37.754	37.755
448.140	8.4450	8.4462	320.24	320.34	37.763	37.763
448.173	7.7314	7.7290	300.70	300.75	34.277	34.276
448.168	7.7310	7.7292	300.70	300.76	34.219	34.218
448.166	7.7312	7.7295	300.72	300.77	34.265	34.265
448.173	7.1790	7.1769	280.72	280.65	31.078	31.077
448.179	7.1799	7.1773	280.73	280.67	31.087	31.086
448.178	6.7437	6.7415	260.32	260.11	28.208	28.207
448.174	6.7436	6.7417	260.33	260.12	28.195	28.194
448.154	6.3988	6.3985	240.49	240.18	25.666	25.666
448.156	6.3990	6.3986	240.50	240.19	25.681	25.681
448.149	6.3986	6.3986	240.49	240.19	25.672	25.672
448.165	6.2461	6.2451	230.47	230.15	24.505	24.505
448.157	6.2458	6.2453	230.49	230.17	24.499	24.499
448.117	6.1047	6.1068	220.92	220.60	23.433	23.434
448.124	6.1054	6.1070	220.94	220.61	23.433	23.434
448.172	5.9637	5.9624	210.50	210.21	22.348	22.347
448.173	5.9638	5.9624	210.51	210.21	22.329	22.328
448.132	5.8300	5.8310	200.77	200.53	21.377	21.378
448.139	5.8304	5.8310	200.77	200.53	21.386	21.386
448.144	5.6914	5.6917	190.39	190.20	20.398	20.398
448.140	5.6913	5.6918	190.41	190.21	20.392	20.392
448.149	5.5516	5.5517	180.07	179.92	19.487	19.487
448.144	5.5515	5.5518	180.08	179.93	19.472	19.472
448.170	5.2679	5.2671	160.05	159.97	17.861	17.860
448.176	5.2682	5.2671	160.05	159.98	17.857	17.856
448.182	4.9488	4.9477	139.90	139.85	16.406	16.405
448.167	4.9487	4.9482	139.91	139.87	16.413	16.412
448.113	4.5702	4.5712	119.47	119.46	15.120	15.121
448.123	4.5708	4.5715	119.49	119.48	15.123	15.124
448.172	4.1373	4.1368	99.823	99.802	14.041	14.040
448.171	4.1375	4.1370	99.830	99.811	14.049	14.048
448.152	3.8798	3.8797	89.740	89.721	13.554	13.554
448.152	3.8797	3.8797	89.742	89.720	13.550	13.550
448.163	3.5160	3.5158	77.019	76.996	12.988	12.988
448.171	3.5161	3.5157	77.013	76.994	12.988	12.987
448.166	3.5067	3.5065	76.710	76.691	12.978	12.978
448.166	3.5064	3.5062	76.703	76.682	12.978	12.978
448.135	3.2458	3.2460	68.540	68.520	12.645	12.645
448.136	3.2459	3.2461	68.541	68.524	12.647	12.647
448.159	2.9144	2.9143	59.028	59.009	12.296	12.296
448.168	2.9147	2.9145	59.034	59.016	12.299	12.299
448.157	2.5406	2.5405	49.292	49.281	11.976	11.976
448.160	2.5404	2.5403	49.285	49.277	11.977	11.977
448.114	2.1128	2.1130	39.195	39.200	11.681	11.682
448.126	2.1126	2.1128	39.199	39.194	11.682	11.683
448.149	2.1136	2.1136	39.218	39.213	11.680	11.680
448.135	1.9287	1.9288	35.146	35.145	11.574	11.574
448.133	1.9283	1.9284	35.135	35.136	11.574	11.574
448.126	1.6801	1.6802	29.916	29.913	11.449	11.450

TABLE 7. *Continued*

T (K)	p (MPa)	$p_{448.15K,\rho_{exp}}$ (MPa)	ρ_{exp} (kg m^{-3})	$\rho_{eos(p,T)}$ (kg m^{-3})	η (μPa s)	$\eta_{448.15\ K}$ (μPa s)
448.129	1.6802	1.6803	29.918	29.915	11.447	11.448
448.157	1.4422	1.4422	25.137	25.137	11.344	11.344
448.165	1.4422	1.4422	25.135	25.137	11.342	11.342
448.186	1.1596	1.1595	19.732	19.731	11.235	11.234
448.182	1.1591	1.1590	19.719	19.723	11.240	11.239
448.093	0.96811	0.96826	16.222	16.223	11.168	11.169
448.132	0.97002	0.97006	16.255	16.256	11.170	11.170
448.132	0.97031	0.97035	16.259	16.261	11.171	11.171
448.150	0.83564	0.83564	13.853	13.855	11.137	11.137
448.150	0.83634	0.83634	13.866	13.868	11.133	11.133
448.177	0.68706	0.68701	11.254	11.261	11.097	11.096
448.176	0.68739	0.68735	11.259	11.267	11.098	11.097
448.175	0.60097	0.60094	9.7844	9.7864	11.077	11.076
448.173	0.60117	0.60114	9.7890	9.7897	11.077	11.076
448.179	0.51768	0.51764	8.3767	8.3777	11.060	11.059
448.173	0.51771	0.51768	8.3774	8.3783	11.057	11.056
448.113	0.36633	0.36636	5.8678	5.8640	11.025	11.026
448.126	0.36720	0.36722	5.8807	5.8781	11.022	11.023
448.137	0.26601	0.26602	4.2282	4.2273	11.008	11.008
448.125	0.26602	0.26603	4.2259	4.2276	11.008	11.009
448.149	0.12754	0.12754	2.0068	2.0071	10.977	10.977
448.143	0.12752	0.12752	2.0068	2.0067	10.980	10.980
448.159	0.064420	0.064419	1.0093	1.0093	*10.966**	*10.966**
448.176	0.064421	0.064417	1.0078	1.0093	*10.966**	*10.965**

*Influenced by slip.

highest densities. Analogously in the case of the equation of state of Miyamoto and Watanabe,[21] the deviations increase up to −1.80% at ρ=460 kg m^{-3} and decrease afresh down to −1.23% at ρ=497 kg m^{-3}. In contrast, for the equation of state of Span and Wagner,[14] the deviations increase up to −0.86% at ρ=420 kg m^{-3}, decrease with further increasing density, change the sign, and achieve their highest positive value with +0.55% at ρ=497 kg m^{-3}. For the reference equation of state of Bücker and Wagner,[1] deviations of ±0,41% appear at most. Figures 4 and 6 make obvious that the trend of the deviations between the experimental and calculated pressure values for the different equations of state is not conform with that between experimental and calculated density values.

Finally, data from the literature measured in the immediate vicinity of the critical point are to be investigated. For this purpose, the experimental pressure values are again considered instead of the experimental densities. In 1949, Beattie et al.[24] reported experimental data measured for 13 isotherms within a temperature interval of 0.55 K including the critical temperature (T_c = 407.81 K) at densities $181 \leq \rho/\mathrm{kg\,m^{-3}} \leq 270$. These data were chosen by Bücker and Wagner[1] to be primary. In contrast, the data of Beattie et al. were not used for developing the equations of state of Younglove and Ely,[20] of Miyamoto and Watanabe,[21] and of Span and Wagner.[14] Figure 7 represents the comparison of the experimental pressure data of Beattie et al. with pressure values calculated from the experimental temperature and density data using the equation of state of Bücker and Wagner. The deviations are within ±0.10%, while most of the data points are even reproduced within ±0.04%. The averaged absolute deviation of 0.015% is to be contemplated in proportion to the uncertainty of the equation of state of 0.5% in pressure stated above for the near-critical region. The huge number of measuring points of Beattie et al. used as primary data by Bücker and Wagner influences distinctly the equation of state in the immediate vicinity of the critical point. A similar result has been received for *n*-butane.[8]

Furthermore, two sets of experimental $p\rho T$ data of Masui et al.[23] determined in the immediate vicinity of the critical point should also be taken into account. These sets were reported in 2006 after development of the discussed four equations of state. The first dataset of Masui et al. concerns seven isotherms, pretty close to the critical point in small intervals of temperature ($407.87 \leq T/\mathrm{K} \leq 407.92$) and of density ($220 \leq \rho/\mathrm{kg\,m^{-3}} \leq 235$). Figure 8 illustrates the deviations of the corresponding experimental pressure data from values calculated using the reference equation of state of Bücker and Wagner.[1] They are between +0.10% and +0.17% with an averaged absolute deviation of 0.14%, about 10 times greater than that for the experimental pressure data of Beattie et al.[24] (see Figure 7). The second dataset of Masui et al., which has already been utilized partially in Figure 5, contains isothermal pressure values at four subcritical and at four supercritical temperatures in the range $405 \leq T/\mathrm{K} \leq 410$ and at densities $184 \leq \rho/\mathrm{kg\,m^{-3}} \leq 265$. As the data for the subcritical isotherms are distinguished by larger uncertainties, as already stated above, only the deviations for the experimental pressure data of the supercritical isotherms are plotted in Figure 8. All of the data points are characterized by deviations ≤ +0.22% with an averaged absolute deviation of 0.17%. In summary, the comparison shown in Figure 8 makes obvious that the two datasets of Masui et al. are in good agreement with the values calculated using the reference equation of state of Bücker and Wagner. The reason for the nearly perfect agreement of the data of Beattie et al. with the reference equation of state of Bücker and Wagner consists in the fact that this dataset was the only in the immediate vicinity of the critical point that could be used for the development of the equation of state. Hence, the uncertainty of the dataset and its weighting do not play a decisive role for the formation of the reference equation of state. The dataset of Beattie et al. is certainly not distinguished by a considerably lower uncertainty than that of Masui et al.

Table 8. Experimental $\eta\rho pT$ Data for Isobutane at 473.15 K

T (K)	p (MPa)	$p_{473.15K,\rho_{exp}}$ (MPa)	ρ_{exp} (kg m^{-3})	$\rho_{eos(p,T)}$ (kg m^{-3})	η (μPa s)	$\eta_{473.15\ K}$ (μPa s)
473.177	30.205	30.198	440.80	440.98	72.532	72.531
473.185	30.208	30.199	440.80	440.99	72.598	72.597
473.149	24.602	24.603	420.26	420.33	64.566	64.566
473.149	24.603	24.603	420.26	420.33	64.694	64.694
473.145	24.604	24.605	420.27	420.34	64.488	64.488
473.155	20.409	20.408	400.22	400.23	57.841	57.841
473.154	20.411	20.410	400.23	400.24	57.828	57.828
473.135	17.150	17.152	379.86	379.89	51.892	51.892
473.142	17.152	17.153	379.86	379.89	51.905	51.905
473.135	14.807	14.810	360.76	360.82	46.984	46.984
473.129	14.808	14.812	360.78	360.84	47.057	47.057
473.130	14.809	14.812	360.78	360.84	46.950	46.950
473.182	12.856	12.852	339.84	339.96	42.303	42.302
473.178	12.856	12.853	339.85	339.96	42.315	42.314
473.173	11.441	11.439	320.05	320.18	38.297	38.297
473.179	11.442	11.439	320.06	320.19	38.275	38.274
473.133	10.317	10.319	299.81	299.91	34.796	34.796
473.131	10.317	10.319	299.82	299.92	34.739	34.739
473.126	10.317	10.320	299.84	299.93	34.790	34.790
473.154	9.4673	9.4669	280.36	280.34	31.749	31.749
473.156	9.4680	9.4674	280.37	280.35	31.740	31.740
473.178	8.7351	8.7329	259.60	259.47	28.766	28.765
473.171	8.7343	8.7326	259.59	259.46	28.799	28.799
473.169	8.7344	8.7328	259.59	259.47	28.796	28.796
473.186	8.1588	8.1562	240.09	239.90	26.322	26.321
473.193	8.1587	8.1557	240.07	239.88	26.301	26.300
473.175	7.8928	7.8911	230.13	229.91	25.172	25.171
473.163	7.8922	7.8913	230.13	229.92	25.161	25.161
473.128	7.6458	7.6472	220.42	220.21	24.118	24.119
473.130	7.6468	7.6480	220.46	220.24	24.118	24.118
473.152	7.4015	7.4014	210.19	209.99	23.028	23.028
473.161	7.4017	7.4010	210.17	209.97	23.015	23.015
473.162	7.1687	7.1681	200.14	199.96	22.045	22.045
473.160	7.1688	7.1683	200.14	199.97	22.021	22.021
473.159	6.9416	6.9411	190.14	190.00	21.102	21.102
473.163	6.9418	6.9412	190.14	190.00	21.099	21.099
473.161	6.7145	6.7140	180.06	179.94	20.213	20.213
473.160	6.7146	6.7141	180.05	179.94	20.206	20.206
473.161	6.4889	6.4884	170.05	169.96	19.371	19.371
473.180	6.4891	6.4878	170.03	169.94	19.373	19.372
473.165	6.2539	6.2533	159.78	159.70	18.565	18.565
473.165	6.2540	6.2535	159.79	159.71	18.562	18.562
473.145	5.7759	5.7761	139.79	139.73	17.130	17.130
473.151	5.7760	5.7760	139.79	139.72	17.128	17.128
473.142	5.2632	5.2634	120.07	120.01	15.875	15.875
473.150	5.2633	5.2633	120.06	120.00	15.877	15.877
473.167	4.4731	4.4728	93.541	93.483	14.438	14.438
473.155	4.4731	4.4731	93.549	93.491	14.416	14.416
473.143	4.4744	4.4745	93.597	93.536	14.425	14.425
473.163	4.3596	4.3594	90.101	90.043	14.258	14.258
473.169	4.3597	4.3593	90.100	90.041	14.257	14.256
473.156	4.0077	4.0076	79.943	79.892	13.790	13.790
473.139	4.0075	4.0077	79.944	79.894	13.790	13.790
473.158	3.6260	3.6259	69.738	69.694	13.359	13.359
473.158	3.6280	3.6279	69.789	69.746	13.354	13.354
473.126	3.1712	3.1715	58.554	58.525	12.933	12.934
473.132	3.1719	3.1721	58.566	58.540	12.932	12.932
473.158	2.7891	2.7890	49.852	49.834	12.634	12.634
473.174	2.7898	2.7896	49.865	49.848	12.636	12.635
473.171	2.3335	2.3333	40.226	40.214	12.335	12.334
473.174	2.3366	2.3364	40.289	40.277	12.337	12.336
473.132	2.0625	2.0626	34.826	34.832	12.185	12.185
473.142	2.0619	2.0620	34.811	34.819	12.188	12.188
473.175	1.7861	1.7860	29.576	29.562	12.050	12.049
473.177	1.7863	1.7861	29.576	29.564	12.054	12.053
473.167	1.5299	1.5298	24.855	24.873	11.945	11.945
473.180	1.5297	1.5296	24.856	24.868	11.935	11.934
473.191	1.5291	1.5290	24.855	24.857	11.941	11.940
473.199	1.2307	1.2305	19.602	19.607	11.829	11.828
473.212	1.2314	1.2312	19.612	19.618	11.834	11.833
473.173	1.1422	1.1422	18.086	18.093	11.807	11.806
473.168	1.1423	1.1423	18.087	18.095	11.800	11.800
473.133	0.94669	0.94673	14.803	14.810	11.745	11.745

TABLE 8. *Continued*

T (K)	p (MPa)	$p_{473.15K,\rho_{exp}}$ (MPa)	ρ_{exp} (kg m^{-3})	$\rho_{eos(\rho,T)}$ (kg m^{-3})	η (μPa s)	$\eta_{473.15\ K}$ (μPa s)
473.128	0.94702	0.94707	14.808	14.815	11.743	11.744
473.157	0.90336	0.90335	14.083	14.092	11.730	11.730
473.150	0.90307	0.90307	14.078	14.087	11.731	11.731
473.165	0.77238	0.77235	11.943	11.949	11.691	11.691
473.151	0.77215	0.77215	11.943	11.946	11.693	11.693
473.121	0.66647	0.66651	10.236	10.244	11.670	11.671
473.128	0.66667	0.66670	10.240	10.248	11.673	11.674
473.138	0.50806	0.50808	7.7331	7.7341	11.634	11.634
473.133	0.50753	0.50755	7.7240	7.7258	11.630	11.630
473.152	0.40691	0.40690	6.1559	6.1564	11.607	11.607
473.154	0.40712	0.40712	6.1582	6.1597	11.606	11.606
473.174	0.26784	0.26783	4.0183	4.0189	11.579	11.578
473.171	0.26791	0.26790	4.0176	4.0199	11.580	11.580
473.143	0.13590	0.13590	2.0172	2.0237	11.559	11.559
473.128	0.13592	0.13592	2.0180	2.0239	11.558	11.559
473.175	0.067964	0.067960	1.0018	1.0080	11.545	11.544
473.177	0.067974	0.067970	1.0034	1.0081	*11.539**	*11.538**

*Influenced by slip.

Viscosity

The experimental values of each isotherm at the nominal temperature T_{nom} were described as a function of the reduced density δ using a power-series representation restricted to the sixth or a lower power depending on the density range and on the reciprocal reduced temperature τ

$$\eta(\tau,\delta)=\sum_{i=0}^{n}\eta_i(\tau)\delta^i,\quad \tau=\frac{T_c}{T},\delta=\frac{\rho}{\rho_c},\qquad \text{with } T_c=407.81\ \text{K},\ \ \rho_c=225.5\ \text{kg m}^{-3} \tag{4}$$

The values of the critical temperature T_c and critical density ρ_c correspond to those given of Bücker and Wagner.[1] The choice of the reciprocal reduced temperature τ instead of the reduced temperature is irrelevant with respect to the use of Eq. 4, but is associated with the application of τ in the fundamental equation of state as well as in a prospective viscosity surface correlation to be generated. In the course of the multiple linear least-squares regression, weighting factors of $(100\,\eta_{exp}^{-1})^2$ were applied to minimize the relative deviations. In the context of the investigation, the appropriate description of the data for a considered isotherm was checked when increasing the order of the power-series expansion. The performance of the representation with Eq. 4 was judged utilizing the weighted standard deviation σ as criterion. The coefficients $\eta_i(\tau)$ of Eq. 4 together with their standard deviations s.d.$_{\eta_i}$ and the weighted standard deviation σ are listed in Table 10.

In the case of the isotherm 410.15 K, it was found that data incorporated from the complete density range $\rho \le 497$ kg m^{-3} are reproduced best using a power series of eighth order, whereas the performance applying power series of sixth and seventh orders is identical. In addition, it was taken into account that a power series of sixth order yields a very reliable result for the coefficient of the initial density dependence, η_1, when comparing with the increments of the η_1 values for the other investigated isotherms (see Table 10). Thus, a power series of sixth order was chosen for the fit to the measured data of the 410.15 K isotherm. However, it became apparent that the data in the density range $0.82 \le \delta \le 1.14$ corresponding to $185 \le \rho/\text{kg m}^{-3} \le 257$ deteriorate considerably the representation of the dataset as a whole. Hence, those specific values were suspended from the fit of the power series of sixth order to the dataset of the isotherm. After all, Figure 9 shows the viscosity of isobutane for the 410.15 K isotherm as a function of density. In the inset of the figure, the effect of the critical enhancement of the viscosity in the near-critical region is clearly illustrated. The excluded viscosity data marked as filled symbols deviate from the power series by +1.39% at maximum, while the maximum appears near to the critical density. The deviations for most of the data points from the fitted values are within ±0.15%. Only a few points show deviations up to ±0.22%, spread over the whole density range.

In summary, the values quoted in Table 10 clarify that for subcritical isotherms power-series expansions up to the third order and for supercritical isotherms such of sixth order are needed for an adequate representation of the data each. The higher order in the case of the supercritical isotherms follows from the larger density range. Increased values of the weighted standard deviation σ occur for the isotherms 405.15, 410.15, and 498.15 K, but due to different reasons: measurements near the phase boundary (405.15 K), investigation in the vicinity of the critical point (410.15 K), and measurements with the apparatus at a considerably high temperature (498.15 K).

The experimental viscosity data of this article are compared with values calculated for the viscosity surface correlation of Vogel et al.[2] utilizing the measured values for temperature and assigned values for density. As the viscosity correlation of Vogel et al. involves the modified Benedict–Webb–Rubin equation of state proposed by Younglove and Ely,[20] the assigned density values were calculated from the experimental temperature and pressure data applying this equation of state. The viscosity correlation of Vogel et al. is based on the residual quantity concept in which the viscosity is considered to be composed of three contributions

$$\eta(T,\rho)=\eta_0(T)+\eta_R(T,\rho)+\eta_c(T,\rho) \tag{5}$$

Here η_0 is the viscosity in the limit of zero density and is only a function of temperature, η_R is the residual viscosity, and η_c is the critical enhancement of the viscosity. The sum of η_0 and η_R corresponds to the background viscosity η_b. The correlation of Vogel et al. includes a contribution for the viscosity in the limit of zero density (see also Küchenmeister and Vogel[15]) but not a separate term for the

Table 9. Experimental $\eta\rho pT$ Data for Isobutane at 498.15 K

T (K)	p (MPa)	$p_{498.15\mathrm{K},\rho_{\mathrm{exp}}}$ (MPa)	ρ_{exp} (kg m^{-3})	$\rho_{\mathrm{eos}(p,T)}$ (kg m^{-3})	η (μPa s)	$\eta_{498.15\ \mathrm{K}}$ (μPa s
498.173	30.274	30.268	419.11	419.34	64.508	64.508
498.172	30.274	30.269	419.11	419.35	64.548	64.548
498.169	30.271	30.267	419.11	419.34	64.559	64.559
498.175	25.606	25.601	400.01	400.17	57.942	57.942
498.176	25.605	25.600	400.01	400.16	57.991	57.991
498.175	25.606	25.601	400.01	400.17	57.934	57.934
498.161	21.715	21.713	379.82	379.94	52.048	52.048
498.169	21.717	21.714	379.83	379.94	52.088	52.088
498.170	21.717	21.713	379.82	379.94	52.082	52.082
498.156	18.700	18.699	359.81	359.93	46.874	46.874
498.159	16.305	16.304	339.52	339.65	42.346	42.346
498.161	16.305	16.304	339.52	339.65	42.366	42.366
498.146	14.481	14.481	319.97	320.10	38.589	38.589
498.147	14.481	14.482	319.97	320.10	38.648	38.648
498.148	14.482	14.482	319.98	320.10	38.618	38.618
498.146	12.971	12.971	299.68	299.78	35.042	35.042
498.146	12.971	12.971	299.67	299.77	34.979	34.979
498.146	12.971	12.971	299.68	299.78	35.011	35.011
498.144	11.783	11.783	279.99	280.01	32.002	32.002
498.141	11.783	11.784	279.99	280.02	31.960	31.960
498.145	10.772	10.772	259.74	259.70	29.172	29.172
498.149	10.769	10.769	259.68	259.65	29.147	29.147
498.133	9.9493	9.9505	240.43	240.35	26.770	26.770
498.133	9.9495	9.9507	240.42	240.36	26.768	26.768
498.143	9.5524	9.5529	230.10	230.00	25.641	25.641
498.144	9.5520	9.5524	230.09	229.99	25.599	25.599
498.143	9.5515	9.5520	230.09	229.98	25.568	25.568
498.144	9.5513	9.5517	230.07	229.97	25.574	25.574
498.139	9.1919	9.1925	220.17	220.07	24.524	24.524
498.140	9.1913	9.1919	220.16	220.06	24.545	24.545
498.138	8.8364	8.8371	209.90	209.81	23.491	23.491
498.139	8.8371	8.8377	209.92	209.83	23.484	23.484
498.139	8.5132	8.5138	200.19	200.12	22.526	22.526
498.141	8.5144	8.5148	200.23	200.15	22.525	22.525
498.172	8.1771	8.1760	189.73	189.69	21.510	21.510
498.169	8.1757	8.1747	189.68	189.65	21.506	21.506
498.151	8.1689	8.1689	189.52	189.47	21.543	21.543
498.152	8.1688	8.1687	189.51	189.47	21.568	21.568
498.145	7.8698	7.8701	180.11	180.07	20.707	20.707
498.142	7.8703	7.8707	180.13	180.09	20.702	20.702
498.129	7.5588	7.5597	170.22	170.20	19.877	19.877
498.130	7.5588	7.5596	170.22	170.20	19.881	19.881
498.155	7.2415	7.2413	160.08	160.07	19.102	19.102
498.157	7.2416	7.2413	160.08	160.07	19.090	19.090
498.161	6.5998	6.5995	139.97	139.96	17.686	17.686
498.164	6.5998	6.5993	139.97	139.96	17.683	17.683
498.143	5.9183	5.9185	119.66	119.65	16.452	16.453
498.146	5.9190	5.9191	119.68	119.66	16.426	16.426
498.146	5.9192	5.9193	119.69	119.67	16.412	16.412
498.187	5.0933	5.0925	97.002	96.987	15.277	15.276
498.189	5.0935	5.0927	97.006	96.992	15.293	15.292
498.166	4.8115	4.8113	89.817	89.807	14.924	14.924
498.166	4.8111	4.8108	89.803	89.795	14.904	14.904
498.172	4.4114	4.4111	80.059	80.053	14.476	14.475
498.151	4.4076	4.4076	79.979	79.971	14.412	14.412
498.150	4.4080	4.4080	79.983	79.980	14.419	14.419
498.153	3.9113	3.9112	68.598	68.599	13.976	13.976
498.153	3.9113	3.9113	68.599	68.600	13.964	13.964
498.152	3.4901	3.4901	59.526	59.534	13.578	13.578
498.153	3.4901	3.4901	59.526	59.534	13.565	13.565
498.156	3.0215	3.0214	50.006	50.025	13.246	13.246
498.157	3.0211	3.0211	50.003	50.018	13.284	13.284
498.157	3.0238	3.0238	50.056	50.071	13.282	13.282
498.134	2.4622	2.4623	39.386	39.403	*13.025**	*13.025**
498.139	2.4626	2.4627	39.395	39.410	*13.125**	*13.125**
498.138	2.4629	2.4629	39.398	39.416	*13.238**	*13.238**
498.153	1.9504	1.9504	30.277	30.298	12.690	12.690
498.152	1.9504	1.9504	30.278	30.299	12.668	12.668
498.140	1.5756	1.5756	23.954	23.971	*12.443**	*12.443**
498.140	1.5753	1.5753	23.947	23.965	*12.427**	*12.427**
498.139	1.5765	1.5765	23.967	23.985	*12.427**	*12.427**
498.152	1.3286	1.3286	19.929	19.943	*12.338**	*12.338**
498.153	1.3287	1.3286	19.929	19.944	*12.334**	*12.334**

TABLE 9. *Continued*

T (K)	p (MPa)	$p_{498.15K,\rho_{exp}}$ (MPa)	ρ_{exp} (kg m^{-3})	$\rho_{eos(p,T)}$ (kg m^{-3})	η (μPa s)	$\eta_{498.15\ K}$ (μPa s
498.146	1.2026	1.2026	17.913	17.931	*12.307**	*12.307**
498.146	1.2020	1.2020	17.906	17.921	*12.314**	*12.314**
498.134	1.0777	1.0777	15.949	15.963	*12.281**	*12.281**
498.134	1.0767	1.0767	15.931	15.947	*12.285**	*12.285**
498.133	1.0760	1.0760	15.922	15.937	*12.285**	*12.285**
498.130	0.94993	0.94997	13.964	13.978	*12.242**	*12.242**
498.130	0.94978	0.94982	13.963	13.975	*12.242**	*12.242**
498.130	0.95004	0.95008	13.969	13.979	*12.243**	*12.243**
498.159	0.81682	0.81681	11.925	11.936	*12.191**	*12.191**
498.162	0.81715	0.81713	11.931	11.941	*12.191**	*12.191**
498.154	0.69883	0.69882	10.139	10.150	12.249	12.249
498.154	0.69910	0.69909	10.142	10.155	*12.195**	*12.195**
498.152	0.69917	0.69916	10.144	10.156	*12.195**	*12.195**
498.138	0.53749	0.53750	7.7328	7.7440	*12.151**	*12.151**
498.137	0.53764	0.53766	7.7374	7.7463	*12.143**	*12.143**
498.134	0.53777	0.53779	7.7420	7.7483	*12.139**	*12.139**
498.148	0.33445	0.33445	4.7647	4.7702	*12.070**	*12.070**
498.147	0.33445	0.33445	4.7670	4.7702	*12.098**	*12.098**
498.147	0.33452	0.33453	4.7670	4.7713	*12.116**	*12.116**
498.147	0.21183	0.21183	2.9991	3.0031	*12.061**	*12.061**
498.148	0.21179	0.21179	2.9999	3.0026	*12.076**	*12.076**
498.149	0.21180	0.21180	2.9983	3.0028	12.138	12.138
498.163	0.14138	0.14138	1.9955	1.9975	*12.431**	*12.431**
498.163	0.14138	0.14138	1.9955	1.9975	*12.420**	*12.420**
498.160	0.071114	0.071113	1.0011	1.0013	12.113	12.113
498.160	0.071121	0.071119	1.0018	1.0014	*12.380**	*12.380**
498.160	0.071118	0.071117	1.0003	1.0014	*12.083*†	*12.083*†

*Suffered from a superposition by an additional precession movement.
†Influenced by slip.

critical enhancement of the viscosity. The residual viscosity is composed of a term of the initial-density dependence and higher-density contributions, which are given as a combination of double power-series expansions in reduced density and reciprocal reduced temperature and of a free-volume term with a temperature-dependent close-packed density. The correlation is valid from the triple-point temperature ($T_{tr,i\text{-}C_4H_{10}}$ = 113.73 K) to 600 K and up to pressures of 35 MPa in accordance with the equation of state of Younglove

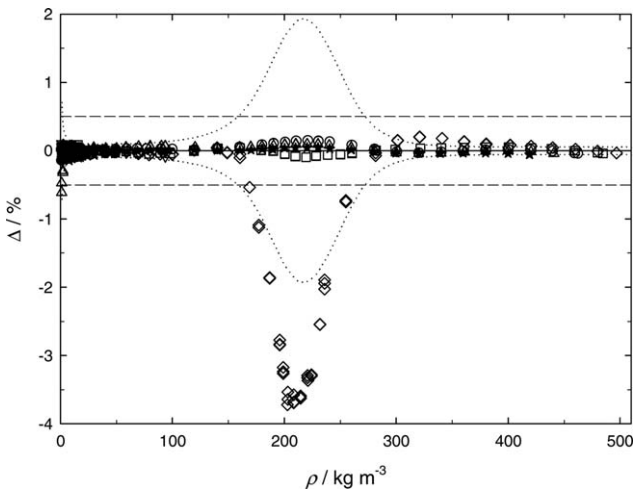

Figure 3. Comparison of the experimental density data ρ_{exp} of this work for isobutane with values ρ_{eos} calculated for the equation of state of Bücker and Wagner[1] using the measured temperatures and pressures as a function of density ρ.

Deviations: $\Delta=100(\rho_{exp}-\rho_{eos})/\rho_{eos}$. ▼, 298.15 K; ▲, 348.15 K; ●, 373.15 K; ▽, 405.15 K; ◇, 410.15 K; □, 423.15 K; ○, 448.15 K; △, 473.15 K; ★, 498.15 K. Uncertainty in density at 410.15 K: · · · · ·, measurement with single-sinker densimeter (Eq. 1); — —, reference equation of state of Bücker and Wagner.

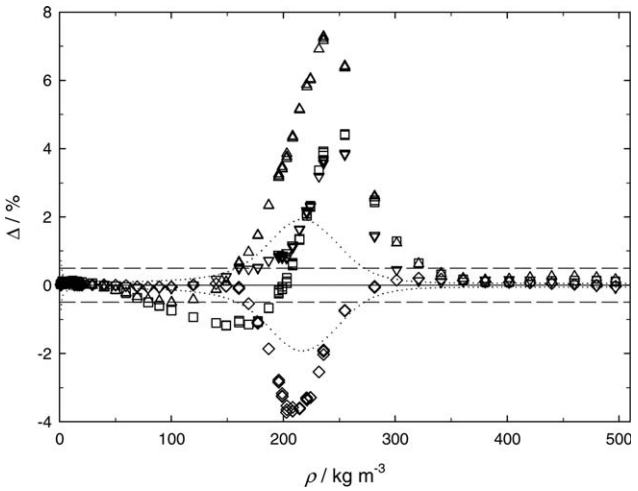

Figure 4. Comparison of the experimental density data ρ_{exp} of this work for isobutane at 410.15 K with values ρ_{eos} calculated for different equations of state using the measured temperatures and pressures, as a function of density ρ.

Deviations: $\Delta=100(\rho_{exp}-\rho_{eos})/\rho_{eos}$. □, equation of state of Younglove and Ely[20]; △, equation of state of Miyamoto and Watanabe[21]; ▽, equation of state of Span and Wagner[14]; ◇, reference equation of state of Bücker and Wagner.[1] Uncertainty in density at 410.15 K: · · · · ·, measurement with single-sinker densimeter (Eq. 1); — —, reference equation of state of Bücker and Wagner.

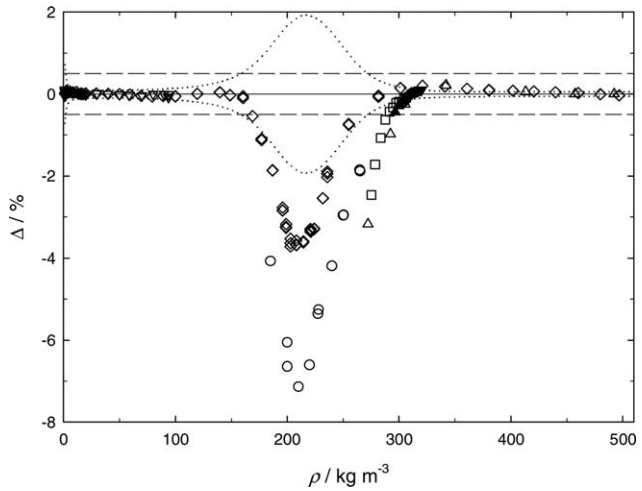

Figure 5. Comparison of experimental density data ρ_{exp} for isobutane between 405 and 410 K and on the saturation curve with values ρ_{eos} calculated for the equation of state of Bücker and Wagner[1] as a function of density ρ.

Deviations: $\Delta=100(\rho_{exp}-\rho_{eos})/\rho_{eos}$. Miyamoto et al.[22]: ▼, 405 K; ▲, 406 K; □, 407 K; △, saturation curve. Masui et al.[23]: ○, 410 K. This work: ▽, 405.15 K; ◇, 410.15 K. Uncertainty in density at 410.15 K: · · · · ·, measurement with single-sinker densimeter (Eq. 1); — —, reference equation of state of Bücker and Wagner.

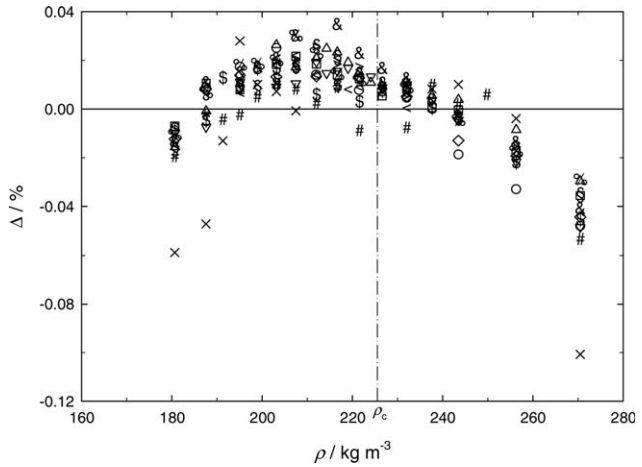

Figure 7. Comparison of experimental pressure data p_{exp} for isobutane of Beattie et al.[24] in the immediate vicinity of the critical point with values p_{eos} calculated for the reference equation of state of Bücker and Wagner,[1] as a function of density ρ.

Deviations: $\Delta=100(p_{exp}-p_{eos})/p_{eos}$. ×, 407.73 K; #, 407.83 K; $, 407.93 K; %, 407.98 K; &, 408.01 K; §, 408.03 K; △, 408.08 K; ▽, 408.10 K; <, 408.11 K; >, 408.12 K; □, 408.13 K; ◇, 408.18 K; ○, 408.28 K.

and Ely. The viscosity correlation is characterized by uncertainties of 0.4% ($298 \le T/\mathrm{K} \le 600, \rho \le 2.91\ \mathrm{kg\,m^{-3}}$) and 1.0% ($273 \le T/\mathrm{K} \le 600, 2.91 < \rho/\mathrm{kg\,m^{-3}} \le 5.81$). In the remaining fluid region in which both the equation of state is valid and primary experimental data are available, the uncertainty was estimated to be 3.0%. These uncertainties were chosen in accordance with those given for the selected reliable experimental datasets. In addition, the uncertainty was assumed to be 4.0%, when primary experimental data do not exist but the equation of state is applicable.

With regard to the critical enhancements of the transport properties of a pure fluid, it is well known that large fluctuations in the order parameter become dominant in the vicinity of its vapor-liquid critical point. The corresponding order

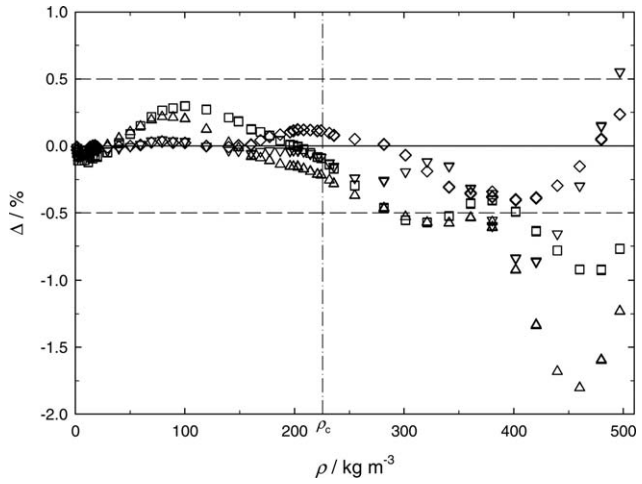

Figure 6. Comparison of the measured pressures p_{exp} of this work for isobutane at 410.15 K with values p_{eos} calculated for different equations of state using the measured temperatures and densities as a function of density ρ.

Deviations: $\Delta=100(p_{exp}-p_{eos})/p_{eos}$. □, equation of state of Younglove and Ely[20]; △, equation of state of Miyamoto and Watanabe[21]; ▽, equation of state of Span and Wagner[14]; ◇, reference equation of state of Bücker and Wagner.[1] — —, uncertainty in pressure of the reference equation of state of Bücker and Wagner in the near-critical region.

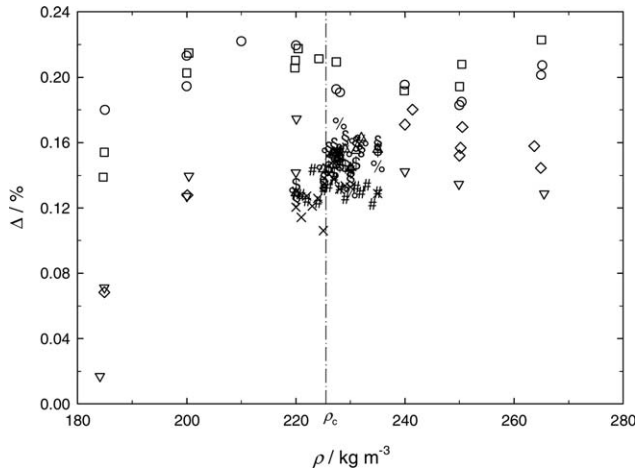

Figure 8. Comparison of experimental pressure data p_{exp} for isobutane of Masui et al.[23] in the immediate vicinity of the critical point with values p_{eos} calculated for the reference equation of state of Bücker and Wagner,[1] as a function of density ρ.

Deviations: $\Delta=100(p_{exp}-p_{eos})/p_{eos}$. First dataset (values taken from Figures 2 and 4 in Reference 23): △, 407.87 K; §, 407.88 K; &, 407.885 K; %, 407.89 K; $, 407.90 K; #, 407.91 K; ×, 407.92 K. Second dataset (values taken from Table 2 in Ref. 23): ◇, 407.89 K; ▽, 408 K; □, 409 K; ○, 410 K.

Table 10. Coefficients of Eq. 4 for the Viscosity Measurements on Isobutane

T (K)	n	ρ_{max} (kg m^{-3})	η_0 (μPa s)	η_1 (μPa s)	η_2 (μPa s)	η_3 (μPa s)	η_4 (μPa s)	η_5 (μPa s)	η_6 (μPa s)	σ
298.15	1	7.98	7.490 ± 0.001	−1.964 ± 0.026						0.011
348.15	3	28.71	8.672 ± 0.001	−1.183 ± 0.109	25.621 ± 2.074	−60.384 ± 10.643				0.023
373.15	3	48.56	9.252 ± 0.001	0.080 ± 0.059	16.472 ± 0.682	−16.673 ± 2.121				0.022
405.15	3	93.75	9.986 ± 0.004	0.886 ± 0.112	13.873 ± 0.698	−4.332 ± 1.148				0.105
410.15	6	496.8	10.106 ± 0.005	1.230 ± 0.104	12.305 ± 0.577	−3.762 ± 1.247	5.291 ± 1.217	−3.207 ± 0.544	0.963 ± 0.090	0.103
423.15	6	484.7	10.392 ± 0.002	1.455 ± 0.032	13.353 ± 0.175	−7.399 ± 0.381	8.844 ± 0.382	−4.620 ± 0.177	1.164 ± 0.031	0.036
448.15	6	462.3	10.963 ± 0.002	1.999 ± 0.045	13.455 ± 0.250	−8.448 ± 0.554	9.512 ± 0.570	−4.680 ± 0.272	1.137 ± 0.049	0.044
473.15	6	440.8	11.536 ± 0.003	2.300 ± 0.062	13.458 ± 0.359	−8.301 ± 0.842	8.687 ± 0.919	−4.013 ± 0.465	0.983 ± 0.088	0.057
498.15	6	419.1	12.102 ± 0.013	2.481 ± 0.245	15.448 ± 1.395	−16.810 ± 3.210	19.929 ± 3.482	−10.362 ± 1.772	2.290 ± 0.340	0.147

parameter is the density ρ at which the range of its fluctuations is characterized by the correlation length ξ. As a consequence, the viscosity η and the thermal conductivity λ diverge at the critical point. The thermal conductivity exhibits a very strong divergence, whereas that of the viscosity is weak and affected only in a small range of temperatures and densities near to the critical point.[25] This behavior of the transport properties is described in the literature by two theoretical approaches (see for instance the discussion in Ref. 26). The dynamic renormalization-group theory is most suitable to predict the asymptotic behavior of the transport properties at the critical point and to establish the understanding of the dynamic scaling and of the universality classes. On the contrary, the mode-coupling theory of critical dynamics has the benefit to be used a little outside the critical region and hence enables to model the crossover from the critical to the near-critical region.

The critical enhancement of the viscosity η_c is proportional to the background viscosity η_b (see Sengers and Luettmer-Strathmann[27])

$$\eta_c = \eta_b[(Q_0\xi)^{z_\eta} - 1] \tag{6}$$

Here, Q_0 and z_η correspond to a system-dependent amplitude and a universal critical exponent. Equation 6 clarifies the behavior of the viscosity when asymptotically approaching the critical point. A nonasymptotic model is required which enables to form the crossover from the asymptotic singular behavior to the regular one corresponding to the background viscosity far away from the critical point. Such a model is worthwhile to be applied not only for the thermal conductivity but also for the viscosity.[27] A simplified closed-form solution of the mode-coupling equations was developed by Bhattacharjee et al.[28] and recently used for the calculation of the critical enhancement of the viscosity of water to generate a new viscosity surface correlation for the International Association for the Properties of Water and Steam.[29]

The comparison between the experimental data of this article and the viscosity surface correlation of Vogel et al.[2]

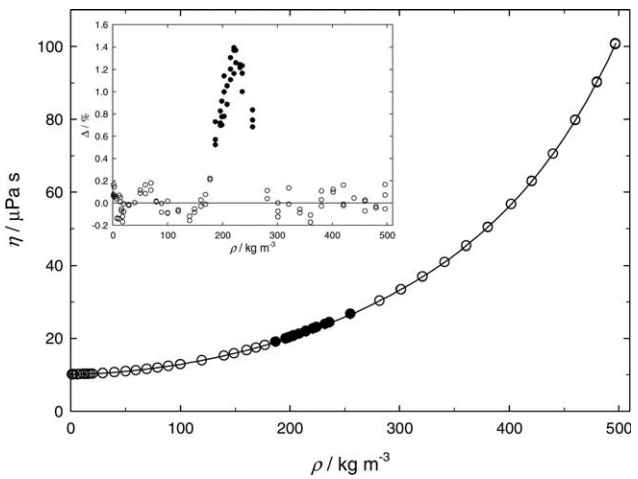

Figure 9. Viscosity of isobutane at 410.15 K as a function of density ρ. ○, measured data η_{exp}; ●, measured data η_{exp} influenced by the critical enhancement; ––, fitted values η_{fit} according to a power-series expansion of sixth order in the reduced density δ (Eq. 4, Table 10).

Deviations in the inset: $\Delta = 100(\eta_{exp} - \eta_{fit})/\eta_{fit}$.

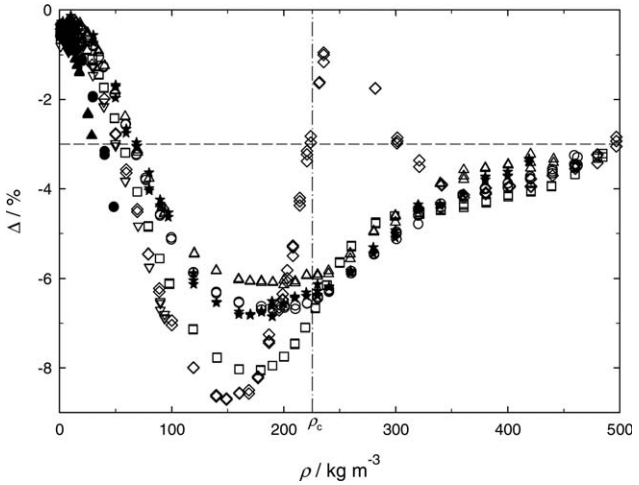

Figure 10. Comparison of experimental viscosity data η_{exp} for isobutane with calculated values η_{cor} using the correlation of Vogel et al.[2] and measured values for temperature and assigned density values, calculated from experimental pressures and temperatures using the equation of state of Younglove and Ely.[20]

Deviations: $\Delta=100(\eta_{exp}-\eta_{cor})/\eta_{cor}$. ▼, 298.15 K; ▲, 348.15 K; ●, 373.15 K; ▽, 405.15 K; ◇, 410.15 K; □, 423.15 K; ○, 448.15 K; △, 473.15 K; ★, 498.15 K. — —, uncertainty of the correlation of Vogel et al.

is illustrated in Figure 10. The figure makes evident that all experimental data are smaller than the values calculated from the viscosity correlation. Thus, negative deviations yield for all isotherms. For the lowest densities $\rho \leq 2.91\ \mathrm{kg\,m^{-3}}$, the deviations are −(0.30 to 0.81)%, larger than the uncertainty of the correlation (0.4%). In the following density range $2.91 < \rho/\mathrm{kg\,m^{-3}} \leq 5.81$, the deviations amount to −(0.26 to 0.72)% and are smaller than the uncertainty (1.0%). Generally, the deviations increase strongly with increasing density for all isotherms. The maximum deviations for the subcritical isotherms occur at the maximum density each and exceed the uncertainty of the viscosity correlation (3.0%) at 373.15 K for densities $\rho \geq 40.1\ \mathrm{kg\,m^{-3}}$ (maximum: −4.41%) and at 405.15 K for densities $\rho \geq 49.9\ \mathrm{kg\,m^{-3}}$ (maximum: −6.89%). The deviations for the supercritical isotherms pass through a minimum. This occurs at $\rho=149\ \mathrm{kg\,m^{-3}}$ for the first supercritical isotherm 410.15 K and achieves −8.71%. For the four higher isotherms, the respective minimum appears in the range $180 \leq \rho/\mathrm{kg\,m^{-3}} \leq 200$ with deviations of −(8.06 to 6.14)%. Even at the highest densities $\rho=(419\text{ to }497)\ \mathrm{kg\,m^{-3}}$, the deviations amount to −(3.48 to 2.84)%, except for two measuring points at 410.15 K, larger than the uncertainty of the correlation. It is to emphasize that the deviations for the 410.15 K isotherm become smaller in the density range $187 \leq \rho/\mathrm{kg\,m^{-3}} \leq 321$, attaining a local maximum of −0.95% at $\rho=236\ \mathrm{kg\,m^{-3}}$. This is in contrast to the trend of the other supercritical isotherms but in accordance with a critical enhancement of the viscosity. Figure 9 has already made obvious that the isotherm 410.15 K is characterized by a critical enhancement, as the deviations of the data in the near-critical region, excluded from the fit of the power series of sixth order to the other data of this isotherm, come up to +1.39% at maximum near the critical density. The enhancement following from Figure 10 is distinctly larger than that illustrated in Figure 9. The reason for that consists in the differences of the used density values, the experimental density data of this work in Figure 9 and the density values calculated with the equation of state of Younglove and Ely[20] in Figure 10 (see also Figure 4). Finally, when comparing the new experimental data with the viscosity surface correlation of Vogel et al., it has to be considered that the experimental data base in the density region $100 < \rho/\mathrm{kg\,m^{-3}} < 300$ was very small at the time of developing the correlation.

Moreover, the new experimental data of this work are contrasted with the older viscosity correlation of Younglove and Ely,[20] the validity range of which extends from the triple-point temperature to 600 K and up to pressures of 35 MPa, again in accordance with the simultaneously proposed equation of state.[20] This viscosity correlation employs also the residual quantity concept, including a contribution for the viscosity in the limit of zero density but not a separate term for the critical enhancement of the viscosity. The residual viscosity considers simply a temperature-independent value as term for the initial-density dependence, whereas an empirical approach with exponential terms was used for the higher-density contributions. The viscosity correlation is distinguished by an uncertainty of 2% overall in the fluid region and of 10% in the near-critical region. To calculate the viscosity values for the correlation, the measured experimental temperatures and assigned density values, calculated from the experimental temperature and pressure data applying the equation of state of Younglove and Ely, were utilized. The deviations of the present viscosity data from the values calculated from the correlation are shown in Figure 11. The figure illustrates that for all isotherms at low and moderate densities $\rho \leq 200\ \mathrm{kg\,m^{-3}}$ only negative deviations occur and that the uncertainty of the correlation is already exceeded at

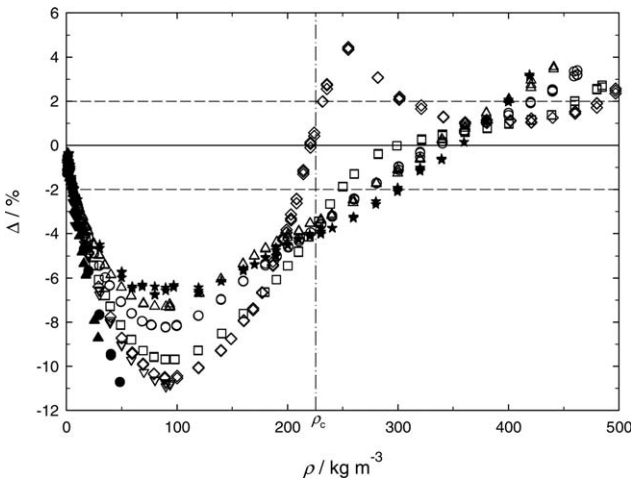

Figure 11. Comparison of experimental viscosity data η_{exp} for isobutane with calculated values η_{cor} using the correlation of Younglove and Ely[20] and measured values for temperature and assigned density values, calculated from experimental pressures and temperatures using the equation of state of Younglove and Ely.[20]

Deviations: $\Delta=100(\eta_{exp}-\eta_{cor})/\eta_{cor}$. ▼, 298.15 K; ▲, 348.15 K; ●, 373.15 K; ▽, 405.15 K; ◇, 410.15 K; □, 423.15 K; ○, 448.15 K; △, 473.15 K; ★, 498.15 K. — —, uncertainty of the correlation of Younglove and Ely.

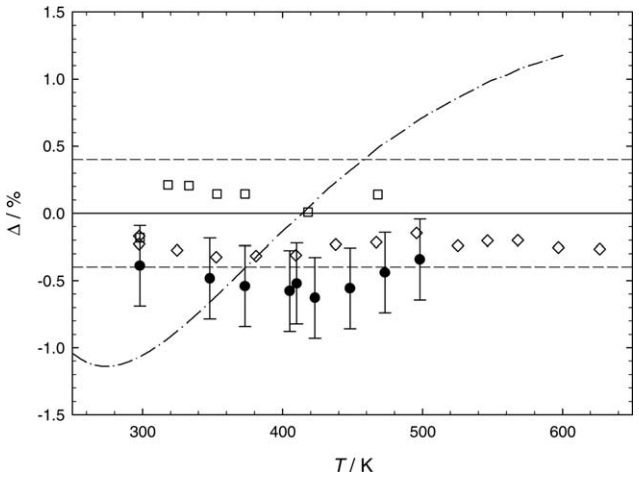

Figure 12. Comparison of experimental viscosity data η_{exp} and of viscosity values calculated from correlations of the literature η_{cor} at low densities and in the limit of zero density, respectively, with calculated values using the correlation of Vogel et al.,[2] $\eta_{cor,Ref.\ 2}$, as a function of temperature *T*.

Error bars: ±0.3% (plotted for the experimental data of this work). Deviations: $\Delta=100(\eta_{exp/cor}-\eta_{cor,Ref.\ 2})/\eta_{cor,Ref.\ 2}$. Experimental data: □, Abe et al.[30] (atmospheric pressure); ◇, Küchenmeister and Vogel,[15] corrected (see Table B.12 in Ref. 31); ●, this work. Correlation: –·–, Younglove and Ely.[20] — —, uncertainty of the correlation of Vogel et al. at low density.

densities $\rho > 5\ \mathrm{kg\,m^{-3}}$. For the four subcritical isotherms, the deviations increase with increasing density and achieve their maximum at the highest density each (one exception: second-highest density at 405.15 K): −3.62% at $\rho=7.97\ \mathrm{kg\,m^{-3}}$ (298.15 K), −8.71% at $\rho=28.7\ \mathrm{kg\,m^{-3}}$ (348.15 K), −10.7% at $\rho=48.5\ \mathrm{kg\,m^{-3}}$ (373.15 K), and −10.9% at $\rho=89.9\ \mathrm{kg\,m^{-3}}$ (405.15 K). The deviations of the five supercritical isotherms 410.15 to 498.15 K pass at densities $\rho=(90\pm1)\ \mathrm{kg\,m^{-3}}$ through minima, whose values decrease with increasing temperature from −10.5 to −6.44%. Then, the deviations decrease with further increasing density, change their sign, and achieve at the highest densities ($\rho=497\ \mathrm{kg\,m^{-3}}$ to $\rho=420\ \mathrm{kg\,m^{-3}}$) the highest positive values with +2.57 to +3.56%. An exception is the isotherm 410.15 K, for which the largest positive deviation +4.55%, that means a maximum, occurs at $\rho=255\ \mathrm{kg\,m^{-3}}$ near to the critical density. This maximum deviation exceeds those of all other supercritical isotherms in this region by about (5.6 to 8.6)% and is concerned with the critical enhancement of the viscosity. The reason for the large difference in the deviations related to that of the other isotherms does not only consist in that the viscosity correlation of Younglove and Ely does not consider the critical enhancement but also in the calculated densities using the equation of state of Younglove and Ely (see the paragraph above). Remarkably for all investigated isotherms, the deviations at densities $\rho > \rho_c$ are smaller than those at densities $\rho < \rho_c$. The bad description which occurs at densities $\rho < 100\ \mathrm{kg\,m^{-3}}$ may be caused by the poor data basis available at the time when Younglove and Ely developed their correlation. Finally, it has to be stated that the viscosity surface correlation of Younglove and Ely is not suitable to represent the experimental data of this work within the uncertainty of 2% estimated for the correlation.

Furthermore, Figure 12 displays a comparison of the viscosity data of this work extrapolated to the limit of zero density (η_0 values of Table 10) with values calculated from the viscosity surface correlation of Vogel et al.[2] The values for the correlation of Vogel et al. are characterized by an uncertainty of 0.4% in the low-density region, while the plotted error bars represent the assumed experimental uncertainty (0.3%). The deviations are between −0.34 and −0.63%, hence the experimental data and the calculated values agree within their mutual uncertainties. In addition, reevaluated data of Küchenmeister and Vogel[15] (see Table B.12 in Ref. 31), which were also extrapolated to the limit of zero density, are presented in the figure. These values deviate by approximately −0.25% from the calculated values of Vogel et al. but exhibit a very good agreement with the temperature function of the viscosity correlation of Vogel et al. The reason for that is that Vogel et al. used the uncorrected and to the limit of zero density extrapolated data of Küchenmeister and Vogel when generating their viscosity surface correlation. The reevaluation of the data determined by Küchenmeister and Vogel applying an oscillating-disk viscometer concerns the calibration of the viscometer. For the recalibration, a value for the zero-density viscosity of argon at room temperature, theoretically calculated with an uncertainty of 0.1% from an *ab initio* potential energy curve for the argon atom pair on the basis of the kinetic theory of dilute gases by Vogel et al.[32] was applied, whereas the viscometer was calibrated originally with a reference value of Kestin et al.[33] from 1972, nowadays considered to be out of date. Old and new reference values differ at 298.15 K by 0.217%, which explains the shift of the reevaluated data. Details regarding the correction of the reevaluated data has been described elsewhere.[31] Moreover, Figure 12 shows a comparison of values calculated from the correlation of Younglove and Ely[20] with those for the correlation of Vogel et al. Differences of $> \pm 1\%$ make obvious that completely different data sets were used for the development of the contribution for the viscosity in the limit of zero density in both correlations. Note that the correlation of Younglove and Ely, generated at NIST, Boulder, is probably based on data measured in the group of Kestin et al. To give an example of this, deviations of data determined at atmospheric pressure by Abe et al.[30] in the group of Kestin et al. are also illustrated in Figure 12.

Conclusions

New quasisimultaneous measurements of viscosity and density on gaseous isobutane were performed in large pressure and temperature ranges using an apparatus combining a vibrating-wire viscometer and a single-sinker densimeter. Nine isotherms were investigated for temperatures between 298.15 and 498.15 K at pressures up to 93% of the saturation pressure for subcritical isotherms or up to 30 MPa for supercritical isotherms. The relative standard uncertainties are 0.1% at $\rho > 15\ \mathrm{kg\,m^{-3}}$ for density and (0.25 to 0.3)% for viscosity. The reason to employ such a combined apparatus is that density values are always needed to evaluate viscosity from the corresponding measurements and that a low uncertainty in viscosity follows from one in density.

The density data were compared with values calculated for the reference equation of state of Bücker and Wagner[1]

using the experimentally obtained values for pressure and temperature. The deviations in density from the reference equation of state are within ±0.1%, excluding the low-density and the near-critical regions. However, deviations up to −3.7% occur for the near-critical region of the isotherm 410.15 K, next to the critical temperature. These deviations exceed the experimental uncertainty of the single-sinker densimeter including the allocation errors for temperature and pressure at this temperature (1.93%), even if the effect of impurities of the used sample is additionally considered (2.27%). The comparison of the experimental density data for the near-critical isotherm 410.15 K was extended to values calculated from the older equations of state of Younglove and Ely,[20] of Miyamoto and Watanabe,[21] and of Span and Wagner[14] and reveals a reasonable agreement within ±0.75% at densities $\rho \leq 100\ \mathrm{kg\,m^{-3}}$ and $\rho \geq 321\ \mathrm{kg\,m^{-3}}$, whereas in the near-critical region large deviations of +(3.9 to 7.3)% occur. New experimental density data of Miyamoto et al.[22] and of Masui et al.,[23] measured between 405 and 410 K after development of the reference equation of state of Bücker and Wagner, lead to deviations from the reference equation, which are in accordance with the density data of this work. Hence, it can be concluded that all new data support a further improvement of the currently used reference equation of state.

An analysis of the primary datasets used by Bücker and Wagner[1] for developing their reference equation of state made obvious that in the immediate vicinity of the critical point older experimental data of Beattie et al.[24] were included, whereas these data were not considered for the other equations of state. The uncertainty in pressure of 0.5% estimated for the equation of state of Bücker and Wagner in the near-critical region is a good deal larger than the deviations of ±0.04% resulting for most of the pressure data of Beattie et al. when comparing with the equation of state. The uncertainty of the data of Beattie et al. and their weighting are not so important for the development of the equation of state, but rather that they are the only in the immediate vicinity of the critical point. This leads to an overestimation of them and consequently to a poor description of other experimental data somewhat away from the critical point.

A fit of a power-series expansion of sixth order in the reduced density δ to the experimental viscosity data of the 410.15 K isotherm made evident that the values in the density range $0.82 \leq \delta \leq 1.14$ deteriorate considerably the representation of the dataset as a whole. After eliminating these data from the fit, they deviate from the power series by about +1.4% at maximum and establish the critical enhancement of the viscosity with regard to sign and magnitude.

The new viscosity data of this article were compared with the viscosity surface correlation of Vogel et al.[2] and with the older one of Younglove and Ely.[20] Both correlations utilize, for calculating required density values from the experimental temperature and pressure data, the modified Benedict-Webb-Rubin equation of state proposed by Younglove and Ely. The correlations are based on the residual quantity concept, but do not include a separate contribution for the critical enhancement of the viscosity. The deviations from the viscosity surface correlation of Vogel et al. exceed the uncertainty of 3%, stated for medium and higher densities of the correlation, for almost all data of the isotherms $T \geq 373.15$ K at densities $\rho > (40\ -50)\ \mathrm{kg\,m^{-3}}$. The deviations for the supercritical isotherms pass through a minimum, while the 410.15 K isotherm is additionally characterized by a local maximum near to the critical density in accordance with the critical enhancement. There are several reasons for the large deviations from the correlation, particularly for the first supercritical isotherm 410.15 K. On the one hand, only a few primary data points were available in the density range $100 < \rho/\mathrm{kg\,m^{-3}} < 300$ at the time when Vogel et al. developed their correlation. Otherwise, the density values calculated from the outdated equation of state of Younglove and Ely[20] suffered from a large uncertainty. In the case of the correlation of Younglove and Ely, the deviations show a similar pattern but with still larger differences, although its uncertainty was judged to be 2%, lower than that of the correlation of Vogel et al.

As a result of the investigation, the reported new viscosity data are appropriate to diminish the uncertainty of a prospective viscosity surface correlation for isobutane. When generating a new correlation, the contribution for the critical enhancement in the near-critical region should be considered using an adequate approach to model it.

Literature Cited

1. Bücker D, Wagner W. Reference equations of state for the thermodynamic properties of fluid phase *n*-butane and isobutane. *J Phys Chem Ref Data*. 2006;35:929–1019.
2. Vogel E, Küchenmeister C, Bich E. Viscosity correlation for isobutane over wide ranges of the fluid region. *Int J Thermophys*. 2000; 21:343–356.
3. Seibt D. *Schwingdrahtviskosimeter mit integriertem Ein-Senkkörper-Dichtemessverfahren für Untersuchungen an Gasen in größeren Temperatur- und Druckbereichen*. Fortschr.-Ber. VDI, Reihe 6, Nr. 571. Düsseldorf: VDI Verlag, 2008.
4. Wilhelm J, Vogel E, Lehmann JK, Wakeham WA. A vibrating-wire viscometer for dilute and dense gases. *Int J Thermophys*. 1998;19: 391–401.
5. Wilhelm J, Vogel E. Viscosity measurements on gaseous argon, krypton, and propane. *Int J Thermophys*. 2000;21:301–318.
6. Seibt D, Herrmann S, Vogel E, Bich E, Hassel E. Simultaneous measurements on helium and nitrogen with a newly designed viscometer-densimeter over a wide range of temperature and pressure. *J Chem Eng Data*. 2009;54:2626–2637.
7. Seibt D, Voß K, Herrmann S, Vogel E, Hassel E. Simultaneous viscosity-density measurements on ethane and propane over a wide range of temperature and pressure including the near-critical region. *J Chem Eng Data*. 2011;56:1476–1493.
8. Herrmann S, Voß K, Hassel E, Vogel E. Simultaneous viscosity and density measurements on normal butane over a wide range of temperature and pressure including the near-critical region. *High Temp High Pressures*. In press.
9. Bich E, Hellmann R, Vogel E. *Ab initio* potential energy curve for the helium atom pair and thermophysical properties of the dilute helium gas. II. Thermophysical standard values for low-density helium. *Mol Phys*. 2007;105:3035–3049.
10. Klimeck J, Kleinrahm R, Wagner W. An accurate single-sinker densimeter and measurements of the (p,ρ,T) relation of argon and nitrogen in the temperature range from (235 to 520) K at pressures up to 30 MPa. *J Chem Thermodyn*. 1998;30:1571–1588.
11. Lösch HW. *Entwicklung und Aufbau von neuen Magnetschwebewaagen zur berührungsfreien Messung vertikaler Kräfte*. Fortschr.-Ber. VDI, Reihe 3, Nr. 138. Düsseldorf: VDI-Verlag, 1987.
12. Lösch HW, Kleinrahm R, Wagner W. Neue Magnetschwebewaagen für gravimetrische Messungen in der Verfahrenstechnik. In: VDI-Gesellschaft Verfahrenstechnik und Chemieingenieurwesen (GVC). *Jahrbuch 1994*. Düsseldorf: VDI-Verlag, 1994:117–137.
13. Kunz O, Wagner W. The GERG-2008 wide-range equation of state for natural gases and other mixtures: an expansion of GERG-2004. *J Chem Eng Data*. 2012;57:3032–3091.
14. Span R, Wagner W. Equations of state for technical applications. *II. Results for nonpolar fluids*. *Int J Thermophys*. 2003;24:41–109.
15. Küchenmeister C, Vogel E. The viscosity of gaseous isobutane and its initial density dependence. *Int J Thermophys*. 2000;21:329–341.

16. Glos S, Kleinrahm R, Wagner W. Measurement of the (p,ρ,T) relation of propane, propylene, *n*-butane, and isobutane in the temperature range from (95 to 340) K at pressures up to 12 MPa using an accurate two-sinker densimeter. *J Chem Thermodyn.* 2004;36:1037–1059.
17. Glos S, Kleinrahm R, Wagner W. Corrigendum to measurement of the (p,ρ,T) relation of propane, propylene, *n*-butane, and isobutane in the temperature range from (95 to 340) K at pressures up to 12 MPa using an accurate two-sinker densimeter [J. Chem. Thermodyn. 36 (2004) 1037–1059]. *J Chem Thermodyn.* 2006;38:209.
18. Bücker D, Wagner W. A reference equation of state for the thermodynamic properties of ethane for temperatures from the melting line to 675 K and pressures up to 900 MPa. *J Phys Chem Ref Data.* 2006;35:205–266.
19. Lemmon EW, McLinden MO, Wagner W. Thermodynamic properties of propane. III. A reference equation of state for temperatures from the melting line to 650 K and pressures up to 1000 MPa. *J Chem Eng Data.* 2009;54:3141–3180.
20. Younglove BA, Ely JF. Thermophysical properties of fluids. II. Methane, ethane, propane, isobutane, and normal butane. *J Phys Chem Ref Data.* 1987;16:577–798.
21. Miyamoto H, Watanabe K. A thermodynamic property model for fluid-phase isobutane. *Int J Thermophys.* 2002;23:477–499.
22. Miyamoto H, Koshi T, Uematsu M. Measurements of saturated-liquid densities for isobutane at T = (280 to 407) K. *J Chem Thermodyn.* 2008;40:1222–1225.
23. Masui G, Honda Y, Uematsu M. Critical parameters for isobutane determined by the image analysis. *J Chem Thermodyn.* 2006;38:1711–1716.
24. Beattie JA, Edwards DG, Marple S Jr. The vapor pressure, orthobaric liquid density, and critical constants of isobutane. *J Chem Phys.* 1949;17:576–577.
25. Sengers JV. Transport properties of fluids near critical points. *Int J Thermophys.* 1985;6:203–232.
26. Hohenberg PC, Halperin BI. Theory of dynamic critical phenomena. *Rev Mod Phys.* 1977;49:435–479.
27. Sengers JV, Luettmer-Strathmann J. The critical enhancements. In: Millat J, Dymond JH, Nieto de Castro CA, editors. *Transport Properties of Fluids: Their Correlation, Prediction, and Estimation.* Cambridge: Cambridge University Press, 1996:113–137.
28. Bhattacharjee JK, Ferrell RA, Basu RS, Sengers JV. Crossover function for the critical viscosity of a classical fluid. *Phys Rev A.* 1981;24:1469–1475.
29. Huber ML, Perkins RA, Laesecke A, Friend DG, Sengers JV, Assael MJ, Metaxa IN, Vogel E, Mareš R, Miyagawa A. New international formulation for the viscosity of H_2O. *J Phys Chem Ref Data.* 2009;38:101–125.
30. Abe Y, Kestin J, Khalifa HE, Wakeham WA. The viscosity of normal butane, isobutane and their mixtures. *Physica.* 1979;97A:296–305.
31. Herrmann S. *Viskositäts- und Dichtemessungen an n-Butan und Isobutan in größeren Temperatur- und Druckbereichen*. PhD Thesis. Rostock: Universität Rostock, Fakultät für Maschinenbau und Schiffstechnik, 2015.
32. Vogel E, Jäger B, Hellmann R, Bich E. *Ab initio* pair potential energy curve for the argon atom pair and thermophysical properties for the dilute argon gas. II. Thermophysical properties for low-density argon. *Mol Phys.* 2010;108:3335–3352.
33. Kestin J, Ro ST, Wakeham WA. Viscosity of the noble gases in the temperature range 25–700°C. *J Chem Phys.* 1972;56:4119–4124.

Manuscript received Dec. 21, 2014, and revision received Jan. 25, 2015.